Processing of signals detected in calorimeters

N. M. Nikityuk
Joint Institute for Nuclear Research, Dubna

Fiz. Elem. Chastits At. Yadra **25**, 1004–1055 (July–August 1994)

The present status of the methods of detection and processing of electrical and light signals detected in calorimeters is described. The functional schemes and algorithms employed in specialized processors to calculate the energy release of high-energy particles detected by means of calorimeters are described. Also considered are questions of the use of neural networks for triggering, recognition of events with clusters, and also identification of jets. Examples are given of the use of digital signal and wavefront array processors for the construction of multilevel data processing systems in the spectrometers of high-energy physics that contain calorimeters. Examples are considered of the construction of fully programmable first-level triggers for experiments using the recently constructed colliders with 16-ns beam crossing time. It is noted that the method of syndrome coding can be used in some special cases for fast recognition and detection of clusters.

INTRODUCTION

Total-absorption spectrometers (calorimeters), by means of which the energy and sometimes the coordinates of particles (hodoscope calorimeters) are measured, are instruments that are very widely used in the physics of high and superhigh energies. In addition, such detectors are used also under certain conditions to identify particles, and in the future they may also be used to detect particle jets.[1,2] The reason for this is that there exist many physics problems that can be solved using modern colliders and which can be studied by observing in the final state jets, the products of the interaction of quarks and gluons.

The principle of operation of a calorimeter is relatively simple. When high-energy particles are absorbed, secondary particles are produced, and these interact with the material of the detector (Fig. 1).[3] As a result of this absorption, some or all of the energy of the particles is transformed into thermal energy. This is the reason for the name. However, it is very difficult to measure the rise in the temperature, and therefore in the experiments one does not measure the temperature but the signals (mainly electrical and light) that arise as a result of the interaction of the particles with special particle counters (the detectors of the calorimeter) placed in the volume of the calorimeter.

It should be mentioned that Soviet physicists made a decisive contribution to the development of calorimeters. In fact, the first total-absorption spectrometer was used on a Soviet satellite to detect hadrons in cosmic rays.[4] An important stage in the development of total-absorption spectrometers was the creation of the hodoscope calorimeter.[5] In such a device, particle coordinates are determined by measuring the energy release from an electromagnetic or hadronic shower in the transverse section of the calorimeter. The characteristics of hadronic and photon hodoscope calorimeters at superhigh energies (>10 TeV) were considered in Ref. 5. It was noted that in the region of energies of the order of a few teva-electron-volts these detectors are capable of measuring with high accuracy the energy and coordinates of particles and also the masses of unstable particles. The fact that calorimeters have become basic detectors in modern physics is due to a number of their positive qualities:[6]

- It is possible to measure the energy of particles in the range from several mega-electron-volts to the maximum energy achieved in the current accelerators and those under construction. The relative energy resolution increases with increasing energy as $\sigma/E = \text{const}/E^{1/2}$. It is very important that for fixed energy resolution the length of a magnetic spectrometer increases linearly with increasing energy, whereas the length of a calorimeter increases logarithmically.

- By means of calorimeters one can detect neutral particles, both as primary particles and produced among the secondary particles of a shower and contained in it.
- The accuracy of measurement of the coordinates of the axis of a particle shower increases with increasing energy and can be better than 1 mm. Particularly promising are high-precision calorimeters based on scintillating optic fibers and also silicon plates.
- Both the longitudinal and transverse components of particle momenta can be measured. This facilitates the kinematic analysis of events by means of a computer.
- The signals obtained at the calorimeter cell outputs have, as a rule, a short duration (of order 10 ns and less in scintillation calorimeters), and there is therefore a possibility of creating calorimeter triggers by means of event selection.
- When cell calorimeters are used, it is not necessary to use magnets to determine particle momenta.

It is not our task to give a detailed description of the physics of the processes and the great diversity of types and constructions of calorimeters. Several reviews have been devoted to this. For example, Ref. 7 analyzes the mechanism of absorption of particles that pass through the material of a detector in a wide range of energies, gives shower characteristics, considers problems of signal compensation (the ratio of the signals from the electromagnetic and hadronic showers, e/h, must approach unity), and discusses problems of coordinate and angle resolution of the calorimeters and the readout and signal-detection systems. The review of Ref. 8 is completely devoted to a description of the processes and

 1063-7796/94/040428-24$10.00

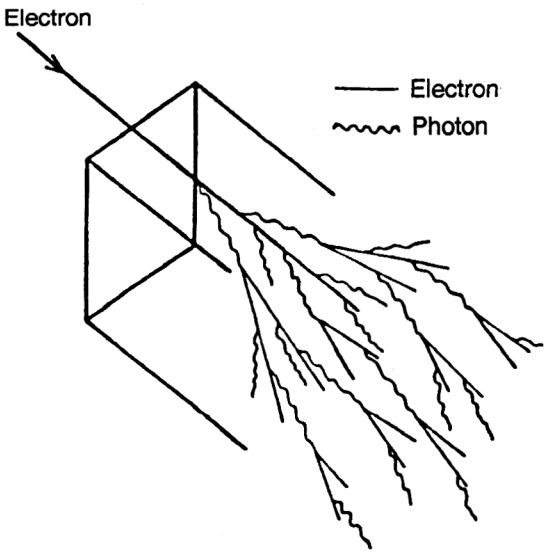

FIG. 1. Example of development of an electron–photon cascade.[3]

characteristics of hadron calorimeters. It briefly considers recent achievements in the methods of hadron calorimeters and the readout and signal-processing methods that are used. The properties of electron—photon calorimeters are described in the review of Ref. 9. There are detailed discussions of the formation of an electromagnetic shower and its characteristics, the general principles of calorimetry, etc. The properties of materials used to make calorimeters are described in the second part of the review of Ref. 10.

The aim of this review is to present, in a form accessible to experimental physicists, the present status within electronic methods of high-energy physics of the methods of formation, detection, and recognition of clusters produced in showers with complicated geometry, for example, in the detection of hadronic jets. In future experiments using colliders such as the LHC, the problem will arise of including data detected in calorimeters in the first-level trigger systems. This is a rather difficult problem in which clusters must be identified by means of extremely fast processor systems that perform billions of operations per second. These and other problems associated with the detection and processing of signals detected in calorimeters require special consideration. The review consists of an introduction, nine sections, and conclusions. In the Introduction we consider the formulation of the problem and the prospects for the development of calorimeters as detectors for experiments in the physics of high and superhigh energies. In the first section, we give some relations associated with measurements of cluster parameters. In the second section, we discuss the way in which signals are obtained in calorimeters and methods used to detect them. The third section is devoted to a description of systems of calibration and monitoring of calorimeters. In Sec. 4 we consider the development of the detection electronics. In the fifth section we describe in detail the most interesting trigger systems used in the experiments that are made. In particular, we consider the most typical schemes of analog and digital processors. Particular attention is devoted to a very promising direction in the development of trigger systems for calorimeters—neural processors and neural networks. The sixth section is devoted to applications in calorimeter trigger systems of signal processors and systolic and wavefront array computational systems. The prospects for the use of such systems in the calorimeter developed for experiments using the Superconducting Supercollider are described in the seventh section of the review. In the eighth section, we consider the fast algorithms used to develop cluster counters. Finally, the ninth section is devoted to a description of special methods of cluster coding on the basis of the method of syndrome coding.

1. BASIC CONCEPTS RELATING TO CALORIMETERS

It should be noted first of all that the construction of hadron calorimeters is based on the same approach as in the case of an electromagnetic hodoscope γ spectrometer.[5] A hadronic shower differs from an electromagnetic shower not only in having greater transverse dimensions but also in the presence of appreciable fluctuations due to correlation processes that determine the number of shower particles. From this there also arises the problem of the ratio e/h in combined calorimeters used to detect not only hadrons but also gamma rays or electrons. The main units of length used to describe the dimensions of electromagnetic showers are its radiation length X_0, which characterizes the longitudinal dimensions, and the Molière radius ρ_M, which determines the development of the shower in the transverse direction. The radiation length is defined as the distance at which an electron whose energy exceeds the critical value has reduced its energy through radiation loss by e times (e is the base of natural logarithms). The radius ρ_M is defined as the ratio X_0/ε_c, where ε_c is the electron energy for which the radiative loss and the loss due to ionization are the same (the critical energy). For this, one uses approximate expressions,[6,7] which depend only weakly on the properties of the material:

$$X_0 = 180A/Z^2(g/\mathrm{cm}^2) \quad \text{and} \quad \rho_M = 7A/Z(g/\mathrm{cm}^2),$$

where Z is the atomic number of the element, g is the density of the material, and A is the atomic weight. Experimental data show that the longitudinal and transverse dimensions of a hadronic shower are determined by the nuclear interaction length λ_{int}. We should mention the modern tendency to develop combined calorimeters with the aim of detecting showers of both types. The standard method for determining the position of the particle that produces a shower is the method of determining the coordinates $\bar{X}$ and $\bar{Y}$ of the "centroid" of the energy released in different cells of the calorimeter with coordinates X_i and Y_i and energy release E_i in a cell:

$$\bar{X} = \frac{\Sigma_i X_i E_i}{\Sigma_i E_i}.$$

In addition, the following shower parameters are measured:[6]

1) The coordinate $X_{\max}$ of the maximum of the shower produced by a particle with energy E (in units of the radiation length X_0):

$$X_{\max} = \ln E/\varepsilon_c - 1.0,$$

where ε_c is the critical energy of the electrons.

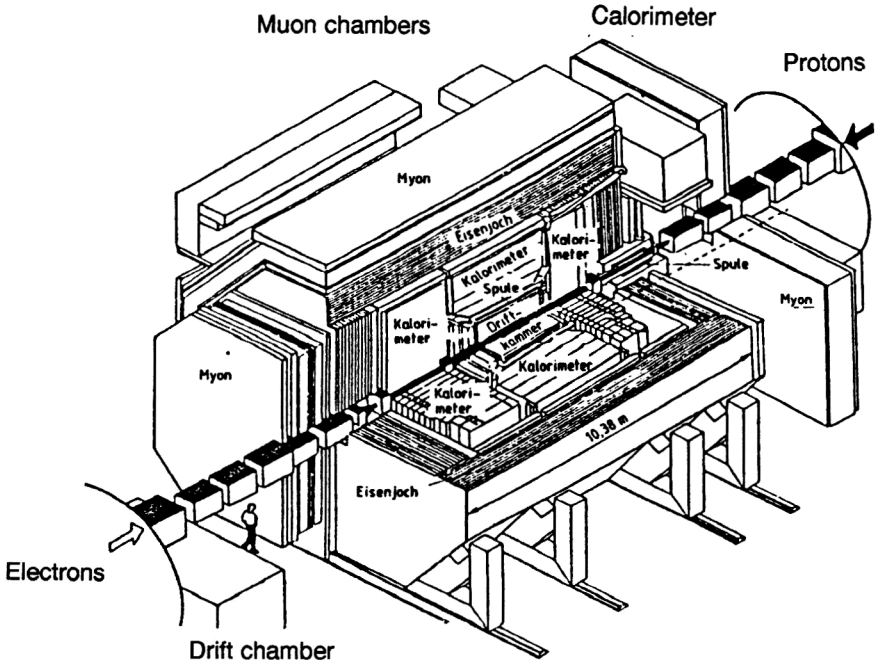

FIG. 2. General form of the ZEUS facility.

2) The total longitudinal depth D after which there is no increase of the detected signal (in units of X_0):

$$D = X_{\max} + 4\lambda_{\text{att}},$$

where λ_{att} is determined by the exponential decay (attenuation) of the shower after the maximum.

3) The transverse dimensions of the shower, which are characterized by the rms magnitude of the energy release relative to the shower axis at the position at which the electrons pass through the critical energy (in units of the radiation length).

Depending on the phase state of the working material of the secondary-particle counters used in a calorimeter, the following types of calorimeter came to be widely used: 1) calorimeters with solid-state counters (scintillator, lead glass, semiconductor); 2) gas-filled calorimeters (drift and geiger tubes and wire chambers are used as counters); 3) liquid calorimeters (liquid scintillator, liquified noble gases). Homogeneous and heterogeneous calorimeters are also distinguished. In a homogeneous calorimeter, the working substance of the secondary-particle counters is simultaneously the material in which all the main processes of interaction of the primary and secondary particles that lead to the formation of the hadronic or electromagnetic shower take place. In this case, the energy of the primary particle is released directly in the working volume of the calorimeter counters.

In a heterogeneous calorimeter, the shower develops mainly in a volume that is insensitive to the particles (for example, in metallic plates). The particle counters are usually distributed uniformly in special cavities within insensitive material, in which a small fraction of the shower energy is released (for example, the counters are placed in gaps between the metallic plates). If a heterogeneous calorimeter consists of a large number of detecting counters, each of which is surrounded by material that is needed for the development of a shower (or contains the material within itself), then such a cellular calorimeter has properties close to those of a homogeneous calorimeter, and in what follows we shall not distinguish these types of calorimeter.

The great diversity of materials and detectors used in calorimeters, and also of the geometries of the calorimeters themselves and of the types of problems that they solve, imposes certain requirements on the detecting electronics and the systems used for preliminary event selection. Most frequently, calorimeters form part of large physics facilities. As an example, Fig. 2 shows the general form of the ZEUS facility,[2] in which a calorimeter is placed not far from the ion tube after a cylindrical drift chamber. Closer to the ion tube there are usually calorimeters with high discreteness of the particle-detecting cells. Facilities containing several calorimeters and having different constructions have long been used, and there are projects for such facilities.

2. SOME METHODS OF OBTAINING SIGNALS IN CALORIMETERS

2.1. Use of scintillating optic fibers

The use of plastic scintillating optic fibers placed in lead matrices (Fig. 3)[11] makes it possible to construct electromagnetic calorimeters with record matter density and good energy and spatial resolution. Table I gives the parameters of some calorimeters of this type (see Ref. 12 and the corresponding references).

In modern scintillation calorimeters, the employed fibers are often wavelength shifters—light reemitters.[13] The main advantage of shifters over ordinary fibers is that they capture and transport the maximum light to a photomultiplier. This is due to the fact that scintillation radiation (of blue color), propagating along a shifter, is transformed into radiation with longer wavelength, usually corresponding to a green or yellow color, which has better conditions for transporting along an optical light tube and can be effectively collected even on

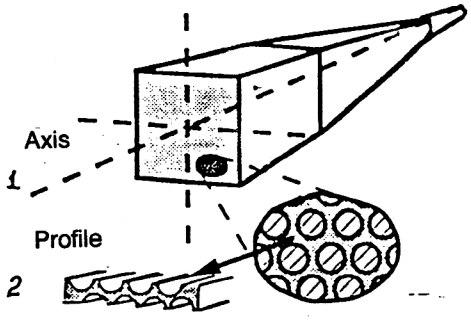

FIG. 3. Calorimeter module including scintillating fibers, lead matrix, and photomultiplier: *1*) module axis; *2*) part of profile of module.

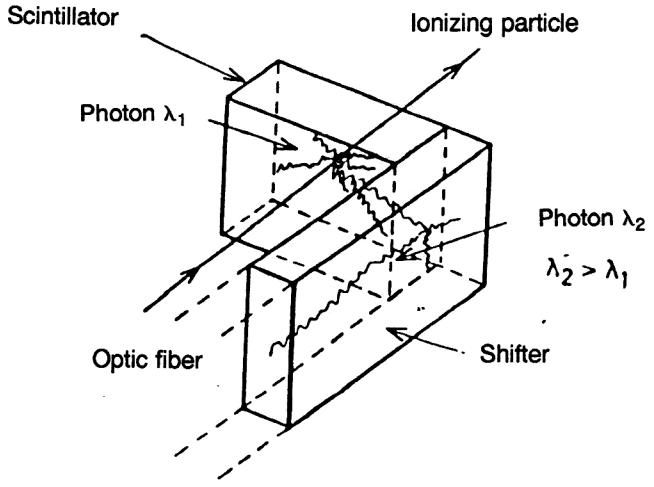

FIG. 4. Explanation of the principle of action of a wavelength shifter.

a photomultiplier with small area of the photocathode. Figure 4 shows the principle of operation of a shifter.[2] An ionizing particle excites in the scintillator light radiation with wavelength λ_1 that is reemitted by means of the shifter as radiation with much longer wavelength λ_2. There are also scintillating fibers that simultaneously perform the function of shifters.[14]

2.2. Signal readout from scintillation calorimeters

By virtue of their well-known valuable properties, and also the good prospects of development associated with the detection of shorter signals and higher resolution, scintillation calorimeters find the widest applications. This can explain the attention devoted to the problem of readout and transmission of light signals. The following elements for readout of light signals are currently used: 1) photomultipliers of various modifications; 2) photodiodes (vacuum and semiconductor); 3) phototriodes; 4) CCD matrices.

The use of photomultipliers

Because of their well-known positive qualities, ordinary photomultipliers are still the most popular devices used in calorimeters. However, there is a facility (DELPHI) in which ordinary photomultipliers are replaced by phototriodes,[15] which have small longitudinal dimensions—of order 60–75 mm—together with a preamplifier and voltage divider. A spatial resolution of 4.4 mm at low noise level has been achieved. In Ref. 16, a module of an electromagnetic calorimeter with longitudinal arrangement of the scintillator and phototriode readout is described. It is noted that calorimeters of the new generation of "spaghetti" type in conjunction with photodiode or phototriode readout can satisfy the requirements imposed on facilities in colliders. Multianode photomultipliers, in which the sizes of the anode segments are adequate for the sizes of the scintillating fibers, can be regarded as very promising devices. A readout system of this type used in a calorimeter is described in Ref. 17. Its features include the following:

- The photomultiplier has 64 readout channels (the size of a readout cell is 5×5 mm), the outputs of which are connected to a multiplexer and then to a charge-sensitive ADC.
- Since the detector channel has a fast response time, it is necessary to determine the delay of signals in order to match them in time with the trigger signal. To this end, a hybrid analog memory device is used.
- A two-channel microcircuit, described in detail in Ref. 18, is used as signal shaper. The use of scintillating fibers and multianode photomultipliers developed by the firm Hamamatsu made it possible to obtain an accuracy of measurement of the shower coordinates better than 900 μm. A schematic diagram of two modules of the calorimeter next to lead-glass plates, in which the shower actually develops, is shown in Fig. 5. Bundles of scintillating fibers are used for high-precision measurement of the position of electromagnetic showers.[19]

TABLE I. General parameters of existing or planned scintillating-fiber calorimeters.

				DELPHI	
Detector	Prototype	Omega	NA38	Prototype	Detector
Year of commissioning	1982	1984	1986	1986	1989
Diameter, mm	0.9	1	1	1	1
Rad. length, cm	1.1/1.6	1.1	0.85	1.3	1.3
Readout	Photomultiplier	Photomultiplier	Photomultiplier	Photomultiplier	Phototriode
σ_E/E	$9.8\%/E^{1/2}$	$10\%/E^{1/2}$	$20\%/E^{1/2}$	$12\%/E^{1/2}$	
Beam energy, GeV	0.04–1	0.5–50	1–1.35	10–50	

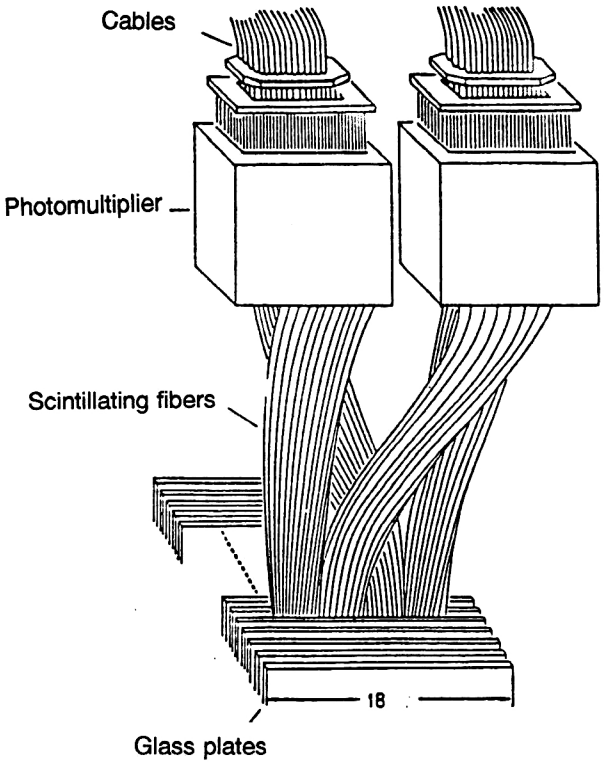

FIG. 5. Calorimeter module based on scintillating fibers and ordinary scintillators in which readout is realized by means of multianode photomultipliers.

Use of vacuum photodiodes for signal shaping

Several studies have been devoted to the use of vacuum photodiodes in calorimeters. In Ref. 20, the following advantages of data readout by means of vacuum photodiodes are noted.

- High stability of the characteristic.
- Low sensitivity to a magnetic field.
- Good energy resolution $22\%E^{1/2}$.
- A high voltage source is not used.
- There is no need for calibration and monitoring in the system.
- The construction is relatively simple.

The use of vacuum photodiodes in a particular device, which uses 1200 detection channels, is described in Ref. 21.

Use of semiconductor photodiodes instead of photomultipliers

The possibility of the practical use of semiconductor photodiodes in calorimeters to replace photomultipliers is being widely investigated in various physical centers. The review of Ref. 22 considers studies devoted to the use of photodiodes with relatively large surface in scintillation counters; attempts to use these began at the beginning of the sixties. In nuclear physics, such counters began to be used in 1969 (Ref. 23). The status of the technology in this field is such that semiconductor photodiodes cannot compete with photomultipliers at energies below 100 keV. The use of photodiodes makes it possible to build compact, cheap, and safe devices. A module of a hadron calorimeter based on a high-density scintillator with photodiode readout and shifter is described in Ref. 24. A photodiode of rectangular shape measuring 30×3.4 mm and with breakdown voltage >30 V was used. The typical readout circuit must include a high-quality amplifier. The calorimeter of Ref. 25 consists of 8000 counters based on CsI crystals, which together with the photodiodes are placed inside a magnetic field of 1.5 T. Satisfactory identification of photons and electrons is achieved. Wide use of scintillating fibers in calorimeters is mainly hindered by the absence of effective readout devices. In this direction, great hopes are associated with the use of avalanche photodiodes.[26] The main shortcoming of ordinary photodiodes is the absence of internal amplification when individual photons are detected. Avalanche photodiodes do not have this shortcoming. A scintillating-fiber hodoscope with readout by means of avalanche photodiodes operating in the geiger regime is described in Ref. 26. For signal amplitude 300 mV the leading edge is 4 ns. The study of Ref. 27 was also devoted to the possible use of avalanche photodiodes for signal readout from scintillating fibers. An avalanche photodiode of diameter 1 mm was directly joined to a scintillating fiber; small light losses were observed. To shorten the photodiode dead time, a specially developed discharge amplifier was used. A dead time of order 50 ns was obtained. However, for experiments using the LHC, this is too long.

Use of CCD arrays

CCD arrays are very promising devices for the readout of signals from scintillating fibers. A feature of the UA2 facility is that the detector based on scintillating fibers is simultaneously used as a track detector and as a counter of electromagnetic showers. In construction, it is a cylinder that is placed between the time-projection chamber and the central calorimeter. The detector consists of 6000 scintillating fibers of diameter 1 mm that form 24 concentric circles with active length 2.1 m (Fig. 6). In turn, the 24 bundles are grouped into eight stereo triplets, each of which contains one layer of scintillating fibers placed parallel to the beam and two layers at a certain angle in order to ensure the detection of data in three projections. In addition, the inner six triplets with stereo angle $\mp15.75°$ are used as track detector. One of the ends of the scintillator is connected to the photocathode of a three-cascade light amplifier, the output of which is scanned by means of a CCD array containing 145×218 cells. Some of them are used as a dynamic memory. The time required for readout of one event is 5.6 ms this being the only shortcoming of CCD arrays as devices for readout of light images.[28]

3. CALIBRATION AND MONITORING SYSTEMS

The unusual complexity of modern physics facilities requires a careful approach to the monitoring and calibration of individual systems and, above all, the numerous counters of a calorimeter. The use of optic fibers significantly raises the efficiency and reliability of such systems. Figure 7 is a schematic diagram of a typical system designed to monitor the amplitudes and time characteristics of scintillation hodo-

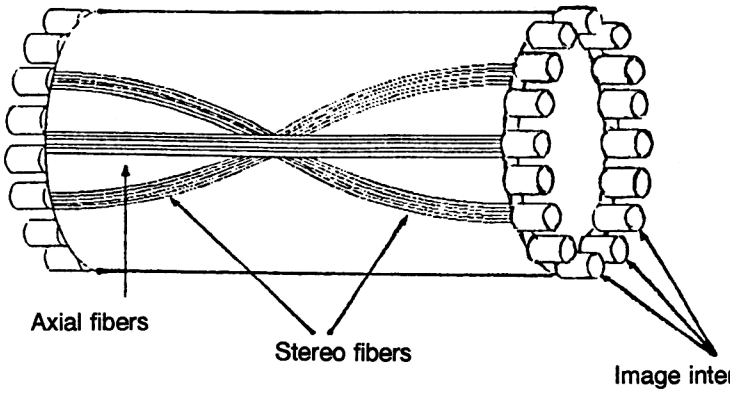

FIG. 6. General form of part of the UA2 detector.

scope systems. The source of powerful light bursts of intensity $>10^{15}$ photons and rise time <1 ns is a laser, whose pulses pass through filters into a bundle of optic fibers. The system also permits calibration of Cherenkov counters and time-of-flight electronics. A laser system[30] has been developed to monitor the stability of the characteristics of the photomultipliers of the electromagnetic calorimeter with accuracy better than 1%.

4. DETECTION ELECTRONICS

The large number of detection channels used both in current and planned experiments with colliding beams at luminosities 10^{32}–10^{33} $cm^{-2}\cdot s^{-1}$ creates not only economic and technical difficulties but also difficulties in the construction of detection electronics that operates reliably under conditions of intense radiation ~20 mrad and neutron flux 10^{14} neutrons/cm^2. These problems arise because the detecting electronics is situated directly at the detector. In addition, since the detector contains liquid at low temperature, there are also stringent requirements on the dissipated power. The signal readout system in liquid calorimeters is relatively simple (Fig. 8).[31] Signals that arise on the electrodes are amplified by means of low-noise amplifiers.

A program of investigations aimed at the development of interference and radiation resistant detection electronics is described in Ref. 32. It is assumed that in the Superconducting Supercollider a liquid-argon calorimeter, which will include an absorber made of heavy metals, will in particular be used. It is calculated that the number of detection channels will be of order $2\cdot10^5$. A detection channel consists of a preamplifier connected directly to a sensitive electrode, a shaper, an analog processor with memory of pipeline type, and an ADC. The J-MOP technology is used to construct the preamplifier; this ensures good resistance to interference and radiation. Investigations showed that after exposure in a neutron flux of 10^{14} neutrons/cm^2 the noise of the bipolar shaper increased by 25%. The strong radiation mainly increases the leakage current. Integrated electronics has also been developed for a "warm" liquid-argon calorimeter[33] containing 9000 detection channels. Amplified and digitized signals are transmitted by means of an optical transmission line to a processor system in the form of a standard FASTBAS for further processing. The topicality of the problem of obtaining a fast signal for ionization (liquid or gas-filled) calorimeters is discussed in Ref. 34. It is shown that the response time of an ionization calorimeter is largely determined by its wave properties. Some recommendations are made for improving the response time of such calorimeters.

Problems associated with making detection electronics for silicon calorimeters are discussed in Ref. 35. Relatively cheap silicon plates of area 25–50 cm^2 that can be used to make silicon calorimeters have been constructed. Two features are taken into account in the construction of the amplifiers—the absence of internal amplification and the relatively large input capacitance. It is planned to use a silicon calorimeter in the SICARO project.[36] Figure 9 shows the general form of a plane of the silicon calorimeter. The plane consists of 48 trapeziform silicon detectors. Each detector

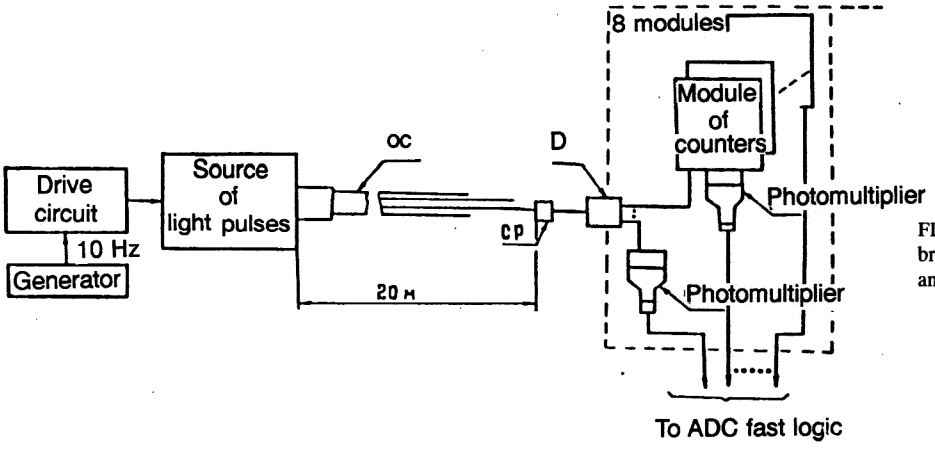

FIG. 7. Block diagram of a typical system for calibrating calorimeters: OC is an optical cable; OJ is an optical connecter; D is a divider.

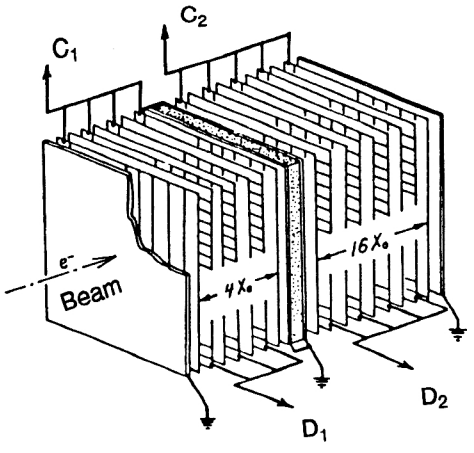

FIG. 8. Typical module of liquid-argon calorimeter; C and D are electrodes.

has a thickness of 400 μm and surface area 28 cm^2.

A radical solution to the problem of the detection of signals read out from counters of scintillation calorimeters is the development of an analog memory based on switched capacitors with 4096 cells[37] and signal sampling frequency up to 100 MHz. The dynamic range, measured at 10 MHz, was 8000:1. The traditional solution to the problem of storing signals was regarded as the use of flash ADCs with subsequent storing of data in a digital memory or using CCD arrays. However, flash ADCs have a small dynamic range (or order 6–8 bits) and, in addition, their use in the case of a large number of channels leads to appreciable power consumption and high cost. With regard to CCD arrays, which have dynamic range 10–12 bits, they require for their operation a high clock frequency and, in addition, their parameters depend on the temperature. The memory array has 16 parallel channels, each of which has a depth of 256 cells. The memory output can be connected to ADCs through a multiplexer. Therefore, such a readout system, being very economic, can at the same time operate in the pipeline regime with high clock frequency in experiments in future colliders.

5. TRIGGER SYSTEMS

Despite certain differences in the formulation of the physical problem as well as in the types and details of the employed calorimeters, several typical methods and approaches are used in the construction of trigger systems; the methods are based on the use of both analog and discrete schemes. It is well known that analog decision devices have a good response time and are economic. Wide use of analog methods of the processing of signals detected in calorimeters is also facilitated by the fact that these signals have a natural character. Therefore, it is not particularly difficult to obtain the sum of a large number of signals by means of analog adders. In addition, in nuclear electronics a tendency has developed toward the use of neural networks, in which analog electronics is predominant. In turn, the use of discrete decision devices increases greatly in connection with the wide use of flash ADCs with digitizing frequency 100 MHz and more and tabulated methods of solution on the basis of fast reprogrammable memories and programmed logic arrays. Digital systems are distinguished by their flexibility, and, in addition, there is a possibility of correcting relatively simply the drift and nonlinearity of the characteristics of the individual cells of the calorimeter. Therefore, both methods have wide prospects for use in the processing of data detected in calorimeters. In the digital scheme, the signals from a photomultiplier are sent after amplification and digitizing to the inputs of a "tree of adders." The energy release of the particles is determined by means of a programmable memory.

5.1. Analog decision devices

A typical analog channel consists of a charge-sensitive amplifier–integrator, a linear gate, and an analog memory with fast clearing. A detailed analysis of the properties of such a channel is made in Ref. 38. If an analog decision device is used, then the output of the analog memory is often connected to a resistive circuit weighted in accordance with a definite rule. Thus, in a modular calorimeter containing 280 proportional tubes such a resistive circuit is used to shape the trigger signal.[39] The calorimeter consists of individual seg-

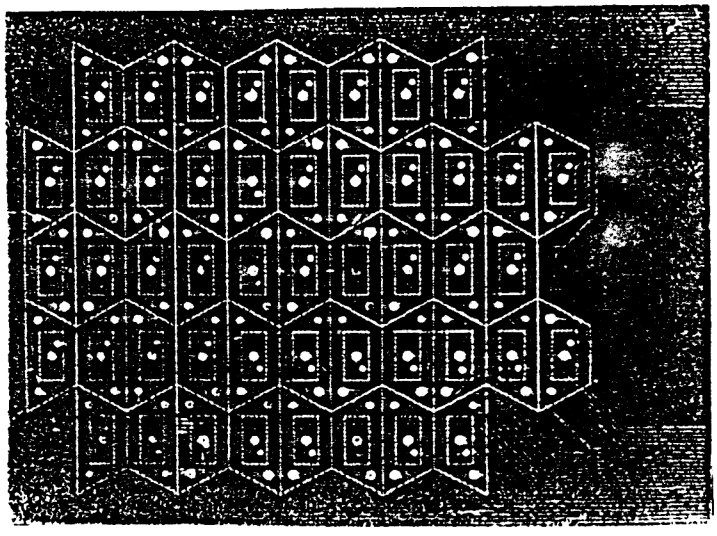

FIG. 9. General form of a plane of the silicon calorimeter. The area of each detector is 28 cm^2.

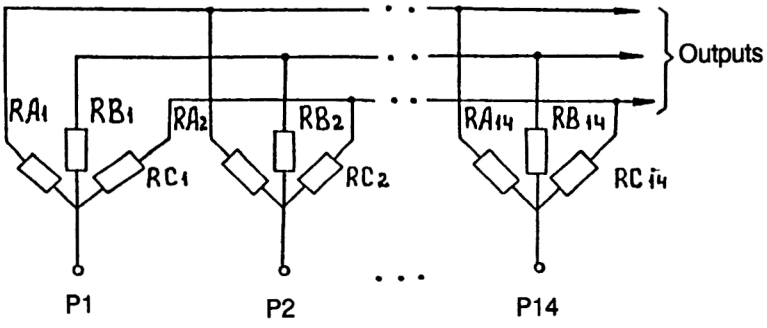

FIG. 10. Part of analog processor made by means of a weighted resistive circuit; P1–P14 are processors.

ments measuring 14×14×30 cm, put together on the basis of the condition that the size of the segments be greater than the expected transverse size of the shower. In its turn, a segment consists of detecting planes intercalated with lead plates (there are 20 planes in all). The weighted resistive circuit is placed in a block together with the detection electronics and the ADC multiplexing devices. In a segment of the calorimeter, each of the 14 signals is split by means of parallel resistors RA, RB, and RC (Fig. 10). All the 14 RA signals, like the RB and RC signals, are sent to the inputs of amplifiers. As a consequence of this, only three signals SA, SB, and SC instead of 14 arrive from each segment. The resistors RA, RB, and RC are chosen in such a way that the three signals contain the maximum of information about the transverse distribution of the shower. At the same time, the condition $1/RA+1/RB+1/RC=1/R=$constant is satisfied. In addition, the following quadratically weighted functions are chosen:

$$f_A=R_0/RA=a(x-c)^2+b,$$

$$f_B=R_0/RB=a(x+c)^2+b,$$

$$f_C=R_0/RC=1-f_A-f_B,$$

where x is the number of the tube, and a, b, and c are constants. The quadratic functions chosen in this manner made it possible to measure the zeroth, first, and second pulses in the energy distribution in the transverse direction in each segment. The use of the analog processor made it possible to distinguish photons from π^0 mesons reliably.

In Ref. 40 there is a description of an analog processor designed for identification of more complicated events with two clusters in a calorimeter containing 132 counters. The amplitudes of the signals obtained at the output of each channel are multiplied by the sine of the angle that characterizes the position of the given counter of the calorimeter relative to the beam axis. A pulse that triggers the facility is produced if the total energy released in a given group of counters exceeds a definite value. The total signal is obtained by means of very fast adders, in which operational amplifiers with transmission band 1.2 GHz are used. The signals that reach the inputs of the adders are coded in advance by means of a coding semiconductor array specially prepared for the experiment. This array makes it possible to code 40 total signals, which are then again added to produce the trigger pulse.

The distinctive feature of the cluster selection device of Ref. 41 is that it is designed to select events with large transverse momenta p_t. The number of neighboring cells of the calorimeter that respond to one photon is 7–10. The following criteria for selecting a useful cluster were used: 1) the calorimeter counter through which the particle passed must be at the center of the cluster; 2) the energy released in this counter must be a maximum compared with the energy released by neighboring counters. At the same time, the signal amplitude must exceed the established threshold of 20 mV. Such a counter is called a peak counter. The energies of all counters of the cluster are then added and multiplied by a correction coefficient in order to obtain the momentum p_t, which is compared with a given value. The readout and detection electronics is based on blocks of the firm LeCroy.

We should mention the original construction of the calorimeter, which makes it possible to simplify considerably the scheme for producing the trigger pulse. The total-absorption spectrometer is designed to study electromagnetic decays of charm states. The calorimeter contains 1280 lead-glass counters. Besides the calorimeter, the facility consists of scintillation hodoscopes, veto counters, track chambers, a segmented Cherenkov counter, and a forward and central electromagnetic calorimeter. The central calorimeter has a cone shape and consists of 1280 counters, each of which "looks" backward in the direction of formation of the interaction vertex. Two arms and the transverse section of the calorimeter are shown in Fig. 11.[42] One arm contains 20 counters, which have different sizes and cover a polar angle 10–70°. In total, there are 64 identical wings, which cover 360°. A unique feature of the calorimeter is that the transverse dimensions of the counters decrease with decreasing polar angle. Accordingly, the diameters of the photomultipliers that are used decrease. The basic principle embodied in the scheme for producing the trigger signal is a step-by-step decrease in the number of signals that participate in the decision making. This is achieved by adding analog signals from neighboring counters into so-called superclusters. A supercluster is obtained by adding the signals from eight counters with the addition of a signal from a neighboring counter. Because of the formation of a jump of the electromagnetic shower in the transverse direction, an appreciable fraction of the released energy is often released at the boundary of the counters. To obtain an effective trigger, sums are formed by overlapping two neighboring counters, and this makes it possible to obtain a maximum of the energy in the supercluster (see Fig. 12). In this way one obtains 40 signals, which are sent to the inputs of discriminators. The two-coordinate readout is organized in a liquid scintillation electromagnetic calorimeter with the aim of selecting showers

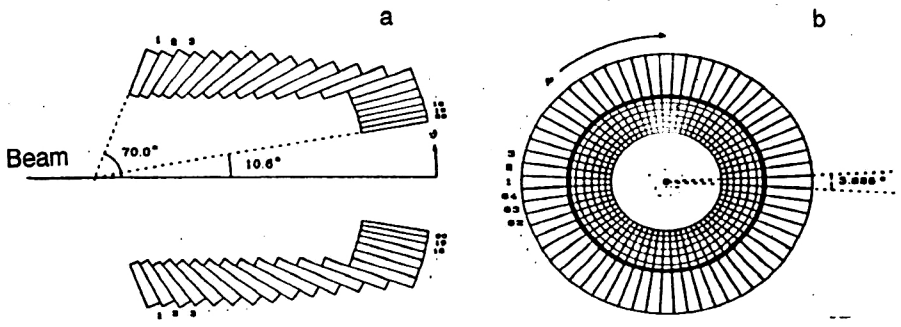

FIG. 11. Two forms of calorimeter in section: a) the number of blocks in the arm covering the angle $\theta=70°$ is shown; b) form of 64 arms arranged along the beam axis.

with large transverse momenta p_t. The electronic selection system contains analog adders at 123 inputs, pulse shapers with integration time 20 ns, fast ADCs with digitizing frequency 100 MHz, and a fast-memory device for table arithmetic. With a total number 3072 of detection channels, the decision time does not exceed 120 ns. Figure 13 shows the scheme of the coordinate system of the calorimeter. Each quadrant is divided into four horizontal and four vertical parts in such a way that 16 cells are used to produce the trigger. The liquid scintillator is in teflon tubes which form a two-coordinate readout system in the XY plane. The signal from the last dynode of each photomultiplier is corrected by means of a resistor in the ratio $1/\sin\theta_y$ or $\sin\theta_z$, where θ_y and θ_z are the angles that determine the position of the photomultiplier relative to the beam axis. Such an approach makes it possible to obtain the energies E_{Tz} and E_{Ty} needed to calculate the values of the transverse energy E_T in accordance with the expression[43]

$$E_T=(E_{Ty}^2+E_{Tz}^2)^{1/2}.$$

5.2. Use of neural networks

It is entirely natural that the use of artificial neural networks, both in pattern recognition systems and in the development of self-teaching parallel computational devices cannot but attract the interest of the developers of apparatus for the physics of high and superhigh energies. It is now possible to note the following directions in the development of the processing of physical information in which the possibilities of using artificial neural networks are investigated.

1) Reconstruction of the tracks of charged particles.[44]

2) Determination of the coordinates of the primary and secondary decay vertices in vertex detectors.[45]

3) Processing of data detected in calorimeters.[46]

4) Identification of particles and jets.[47]

Brief information about neural networks and the problems of their use in experiments in high-energy physics is given in Ref. 48. It is noted that in the future such devices will be able to solve many problems that are impossible for ordinary computers, above all in such fields as pattern recognition and associative methods of information processing. It should be noted that, in contrast to ordinary electronic computing techniques used for the detection and processing

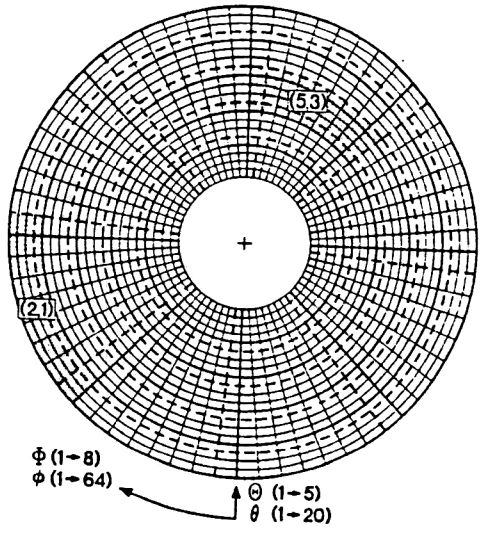

FIG. 12. Explanation of method of shaping supercluster signals.

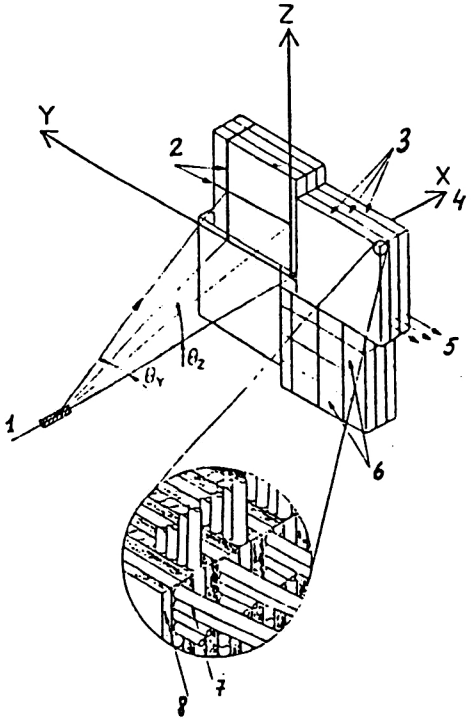

FIG. 13. Schematic diagram of coordinate network of a liquid scintillation electromagnetic calorimeter: *1*) target; *2*) photomultiplier channels; *3*) segments of calorimeter; *4*) beam axis; *5*) light output; *6*) trigger cells; *7*) teflon tubes; *8*) glass plates.

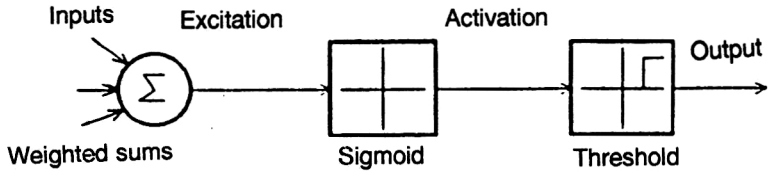

FIG. 14. Sequence of operations in a typical neuron.

of clusters, the use of neural networks at this stage requires much "learning" effort. This problem is intimately related to the choice of the nonlinear function of the network, which depends not only on the formulation of the problem but also on the form of the sigmoid function, which describes empirically the behavior of the neuristor. As an example, Fig. 14 shows the arrangement and sequence of operations in a typical neuron.[49] In Ref. 50, the choice of the nonlinear function is shown for the example of electron identification. A method that is widely used to distinguish electrons from hadrons detected in calorimeters is the covariance-matrix method. In this, the value of the function χ^2 (χ is the standard deviation) is determined. We have

$$\chi e^2=(p-p_e)\mathbf{H}_e(p-p_e) \quad \text{and} \quad Xh^2=(p-p_h)\mathbf{H}_h \times(p-p_h),$$

where p is the momentum, $\mathbf{H}$ is the covariance matrix of the calorimeter, and p_h and p_e are vectors that relate to the amplitude values of the hadron and electron momenta. The problem is to construct a neural network that realizes the given functions. To this end, one constructs a generalized scheme of a neural network, using most often a three-layer network (Fig. 15), which consists of an input, internal, and output layer.[50] The values of the shower energy are sent to the input layer; the central layer is functional and consists of neurons, and two elements at the outputs are used to represent χ^2. A two-layer network has also been used (Fig. 16).[49] One of the layers is used to send input signals, and calculated values are obtained at the output layer. The circles denote neurons, and the numbers on the corresponding lines denote the weight of the links. The next and very laborious stage after the choice of a suitable function is the training process of the network, which involves the development of a corresponding algorithm. Most often the method of trial and error is used by applying both standard and specially developed (for physics experiments) program emulators. It should be noted that the possibilities of artificial neural networks are limited (the number of inputs is 20–60). Therefore, in the construction of an apparatus model the detector is divided into several sections. Part of a calorimeter containing four

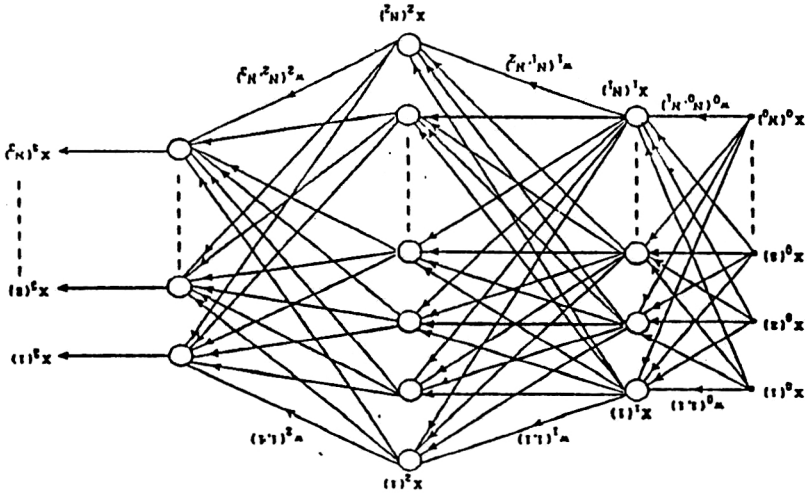

FIG. 15. Example of three-layer perceptron; $X_0(1)-X_0(N_0)$ are inputs; $w_0(1,1)-w_0(N_0,N_1)$ are links; $X_3(1)-X_3(N_3)$ are outputs.

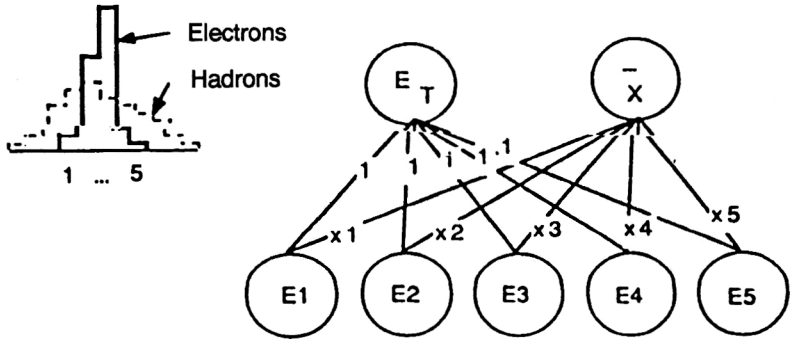

FIG. 16. Two-layer neural network adapted for identification of particles detected by means of a calorimeter; E_1-E_5 are the energies of the individual layers of the calorimeter; E_T is the total cluster energy; $\bar{X}$ is a coordinate.

concentric layers was investigated in Ref. 49. After training, the network identified 90% of the electrons. The algorithm for cluster processing used in Ref. 51 was developed for calculations on a vector computer of pipeline type.

In Ref. 52, data are given on a model of a seven-layer neural network designed for cluster detection and developed at the level of program means. The inputs and outputs of the network are organized in such a way that a definite number of data bytes corresponds to the amplitude values of the calorimeter counters, and an additional data byte is used to measure the cluster width. The algorithm works as follows. Each jth neuron of a given layer is "associated" with eight nearest neighbors of the previous layer and the mean value

$$\text{net}=\left(\sum a_k\right)/8 \quad (k=j)$$

is compared with the quantity a_j obtained at the output of the neuron of the previous layer corresponding to it. If $\text{net}_j > a_j$, then the jth neuron transmits this threshold value to the next layer. In addition, an additional byte of data is transmitted even if the given neuron is inactive. The sensitivities of the layers are different, and this makes it possible to realize the training more accurately.

It has been shown in a number of investigations that the technique of neural networks can be successfully used to distinguish and identify quark and gluon jets generated by the Monte Carlo method in pp and e^+e^- collisions. It is noted[54] that, in contrast to the very complicated and laborious methods of jet identification, the use of neural networks for these purposes has a number of advantages, for example, the possibility of constructing a relatively simple processor, a high degree of parallelism of the calculations, and universality. A standard procedure is used to teach the network, and therefore we consider its essence briefly. The basic concepts are a neuron n_i and the weight of the links ω_{ij}. A neural network without feedbacks has input neurons x_k, internal neurons h_j, and output sites y_i. Each neuron adds the weighted signals and responds in accordance with the sigmoid function

$$g(x)=0.5[1+\tanh(x)].$$

For the internal and output neurons, the following relations hold:

$$h_j=g(a_j/T), \quad y=g(a_i/T),$$

where the "temperature" T determines the slope of the function g, and the weighted sums a_j and a_i are equal to $\Sigma\omega_{jk}$ and $\Sigma\omega_{ij}h_j$, respectively. The purpose of the internal layers is to correlate and create an internal image of the studied event. The training of the network consists above all in changing the weighted sums ω_{ij} in such a way that a given input parameter $x^{(p)}$ ensures growth of the output quantity $y^{(p)}$ to the desired value $t^{(p)}$. In accordance with the trial-and-error principle, it is necessary to minimize the function

$$E=1/2\sum_p \sum_i (y_i^{(p)}-t_i^{(p)})^2.$$

Data for training the network were generated by means of three generators of programs that gave a satisfactory description of the shape of events, their multiplicities, etc., at given energies. After the generation of events, the process of jet identification is initiated by means of a standard cluster search algorithm. Jets between which the angle did not exceed 40° were considered. Events with one and three jets were studied separately. The training procedure is repeated several times for different event images until a satisfactory result is obtained. As criterion for the selection of useful events, use is made of the fact that in the majority of cases the energy of the leading particles in gluon jets is less than in quark jets. In the cited study, the training process consisted of up to 10^5 cycles. The net identified up to 90 jets that had not previously been identified by means of ordinary methods. In Ref. 47, a neural network was used for similar purposes, but the process was studied for pp collisions.

5.3. Digital trigger systems

Irrespective of the specific nature of a facility, digital trigger systems have a number of characteristics: 1) digitization of data by means of fast ADCs with subsequent storing in registers; 2) search for geographical addresses of clusters, for example, the number of a segment or counter containing a local maximum of the energy, calculation of this energy, and comparison with given thresholds; 3) the finding of the coordinates of isolated clusters and calculation of a form factor in order to identify pions and electrons; 4) identification of jets and determination of their coordinates; 5) calculation of the total released energy and the energy released in the transverse direction.

The creation of an effective method for selecting useful events for the UA1 experiment significantly facilitated the successful implementation of this experiment. The development of the calorimeter for the UA1 experiment foresaw various constructional and methodological devices to raise the efficiency of the trigger system. The calorimeter has a cylindrical shape and consists of a supergondola divided into 10 parts along the beam axis and four modules. Around the circumference, the calorimeter is divided into 10 segments measuring 10×10 cm along the front and 40 cm along the beam. In turn, each segment consists of an electromagnetic and a hadronic part. Altogether there are 2560 segments corresponding to supergondolas and 1074 segments that cover the gondola along the beam. This construction of the calorimeter necessitates the presence of individual channels for production of the total trigger signal. For the production of the electromagnetic trigger, only a combination of the electromagnetic counters of four segments is used. The channel of the hadronic calorimeter includes a combination of eight

TABLE II. Number of functional cards.

Analog part of processor	144
Search for electromagnetic clusters	32
Jet detection	16
Strobable adders	18
Arithmetic device	1
Cluster counters	2
Final decision	1

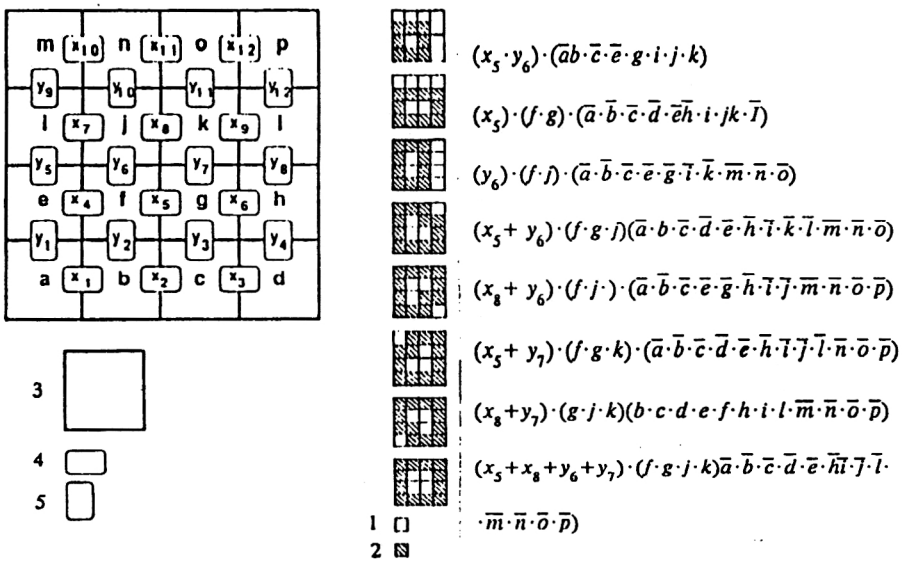

FIG. 17. Explanation of cluster selection algorithm: 1) normal threshold; 2) weak threshold; 3) electromagnetic channel with low threshold; 4) two-input adder-comparator; 5) comparator with high threshold for electrons.

segments. In addition, jets produced in the calorimeter are also selected in accordance with definite criteria. After digitizing, the data from each channel are sent to the inputs of a specialized processor. If one considers the matter briefly, the complexity of the processor can be estimated from the data given in Table II.

We consider briefly the algorithms of the operation of some parts of the processor. Figure 17 gives a diagram that illustrates the method used to look for isolated electromagnetic clusters. Modeling showed that a cluster cannot extend over more than 2×2 neighboring counters. It is therefore unlikely that the counters of the calorimeter that are arranged along the diagonal will respond. It is this that determines the relatively simple cluster search algorithm, which adds the signals from two neighboring counters with allowance for overlap in the horizontal and vertical directions. This function is performed by means of a special module constructed on the basis of programmable logic arrays. Jets are identified somewhat differently if one starts from the fact that the studied jets are more energetic than showers and, in addition, special jet-detecting ("jet brick") counters are foreseen, as we have already said, in the construction of the calorimeter. The processor evaluates an event during 1.5 μs; ensuring operation of the facility without dead time. Figure 18 is a generalized block diagram of the processor system used to analyze clusters and jets in the UA1 experiment.[55]

The processor developed for the DO experiment has a very fast response time (132 ns), which was achieved by the use of the pipeline method of signal processing and a high degree of parallelism.[56] The construction of the processor includes 600 functional cards of six different types. We consider briefly the purpose of these cards. The signals that arrive from the calorimeter counters are amplified and multiplied by means of weighted resistors in order to obtain the value of $E \sin\theta$. In addition, on the first card DACs and parallel ADCs are also mounted, the data from which are stored in registers of pipeline type. This makes it possible to store the "history" of the preceding events.

6. THE USE OF DIGITAL SIGNAL PROCESSORS AND RISK PROCESSORS

Despite the great successes in the construction of ultrafast computers and specialized processors, the growing demands for fast processing of signals detected in calorimeters call for a significant extension of the existing means of computational technology. The effective solution of such a difficult problem is achieved mainly by improving the response time of the logic elements and by using array structures with local connections, systolic and wavefront arrays, the elements of which are specialized processors. It is here appro-

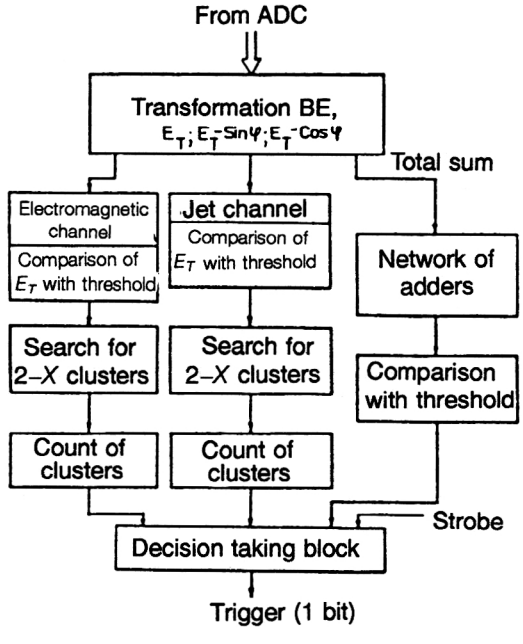

FIG. 18. Generalized block diagram of specialized processor for cluster and jet processing.

priate to mention briefly the architectural conceptions that are used to increase the speed of computers.[57]

Parallel architecture

Parallel computers can be classified in accordance with the type of connections of the processors with the immediate-access memory. Thus, in a classical computer each of the processes can address the common immediate-access memory by means of a multiplex data highway. The shortcoming of this is obvious—it is impossible for even two processes to access the memory simultaneously. The introduction of an additional data highway increases the speed of the system, but conflict situations often arise when processors address the common memory. A significant increase in the speed of the system was achieved by increasing the number of modules of the immediate-access memory and using network switches. However, this greatly increases the cost of the apparatus and the mathematical system provision. Array architecture was more promising. An array processor is an array of processor elements that form linear, orthogonal, hexagonal, treelike, and other connections. It is assumed that each processor has its own immediate-access memory and is connected by means of interfaces and switches to its nearest neighbors. Moreover, multidimensional structures are also developed. Such complicated commutational systems require effective organization of the data flows and the use of new mathematical algorithms. If we speak of the data and command flows, we can identify three different conceptions:

1)To one command flow there corresponds one data flow, as is adopted in the classical von Neumann computer.

2) To one command flow there correspond many data flows.

3) There are many command flows and many data flows.

As will be shown below, simple processors of the first type have been used to process signals, this being due to the simplicity of the connection between them and the rapid development of the technology of ultrafast large integrated microcircuits. It was found that programmable processor modules have a number of advantages compared with specialized signal processors, since the latter can be used to make array processors. For signal processing, two methods of organization of array calculations have been most widely used: the systolic and wavefront array processors.

Systolic processors

A systolic system is a network of processors that rhythmically carry out calculations and "push" data through the computational system. It consists of an array of connected processors (cells), each of which performs simple operations. Because of the regularity of the connections and the synchrony of the calculations, systolic systems have a number of advantages compared with complicated networks of large computers. The information in the systolic array is carried between the cells along a pipeline, which ensures, on the one hand, multiple use of their elements and on the other, the formation of the final result as the pipeline is loaded and accelerated in the same way as the blood pulsates with the systoles of the heart. This is probably the reason for the name

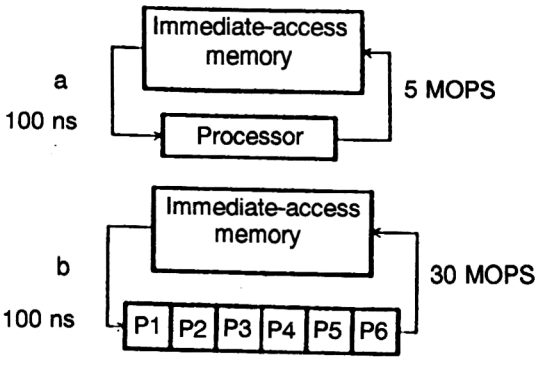

FIG. 19. Scheme of simplest computer with processor and one immediate-access memory (a). Linear systolic system (b) consisting of six processors and one immediate-access memory. P1–P6 are processors.

given to systolic processors.[58,59] Only the processors situated on the boundaries of the array are connected to external devices. A basic advantage of such an approach is the possibility of using a limited number of input–output contact areas for implementation of systolic algorithms. If the processors are organized in the form of an array, the systolic algorithms minimize the delay time associated with data transfer between processors, so that the time cycle can be relatively short. As an example, Fig. 19a shows an ordinary computer consisting of one processor and its corresponding immediate-access memory, and a simple linear systolic system, consisting of six processors and one module of an immediate-access memory (Fig. 19b). Whereas the ordinary processor executes, say, 5 million operations per second (5 MOPS), the six processors in the linear systolic system with one immediate-access memory will be capable of 30 MOPS.[60] The coefficient of acceleration of the calculations K_B is equal to the ratio of the processing time in a single processor to the processing time in the array processor. The systolic array must have the property of linear pipelinability, i.e., the estimate of K_B must increase with increasing number of processor elements. The pipelinability effect is manifested in the fact that the execution of the commands is divided into several stages (microcycles). As a consequence of this, a set of commands is implemented practically in parallel, as is shown in Fig. 20.[61] As an example of the effectiveness of using systolization in two-dimensional computational networks, we consider the two-dimensional operation of multiplying matrices.[58] Let

$$A=[a_{ij}], \quad B=[b_{ij}] \quad \text{and} \quad C=A\times B.$$

Under certain assumptions

$$C=[A_1B_1+A_2B_2+\ldots A_NB_N],$$

where A_iB_i is the outer product. Then the multiplication of the matrices can be done in N recursive steps (Fig. 21). At the same time, the process of calculation has a wavefront nature, since N processing wavefronts are activated.

We consider two examples of the use of systolic processors.

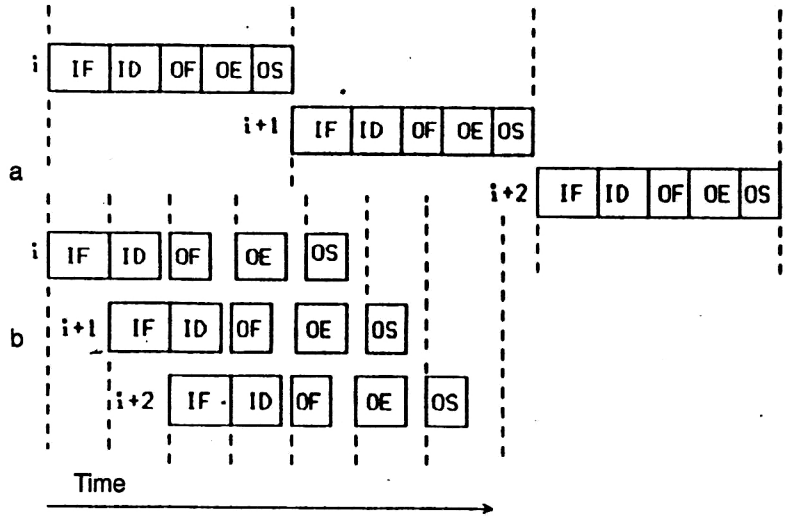

FIG. 20. Example of implementation of three commands: a) sequentially; b) by the pipeline method.

The processor described in Ref. 62 is used in the second level of the trigger system in the NUMASS experiment at CERN. The algorithm of the processor is based on the relation

$$M^2=\Delta tE^2\frac{2}{Lc^3}, \tag{1}$$

where M is the residual mass of a particle, Δt is the difference in the time of flight relative to a particle moving with the speed of light, L is the length of the flight base, and E is the total energy of the particle. This quantity is obtained by adding signals that arrive from the calorimeter in a digitized form obtained by means of ADCs. Figure 22 gives the scheme of calculation of the total energy ΣE_n and the weighted sum

$$\sum_{n=1}^{12} nE_n,$$

where n are the horizontal strips of the calorimeter. To calculate the expression (1), several analog modules are used. It is also important to note that the processor is completely programmable, since it is made using repeatedly erasable gate arrays of the type LCA of the firm XILINX.

Systolic processors, being synchronous in nature, can be successfully included in the trigger systems developed for

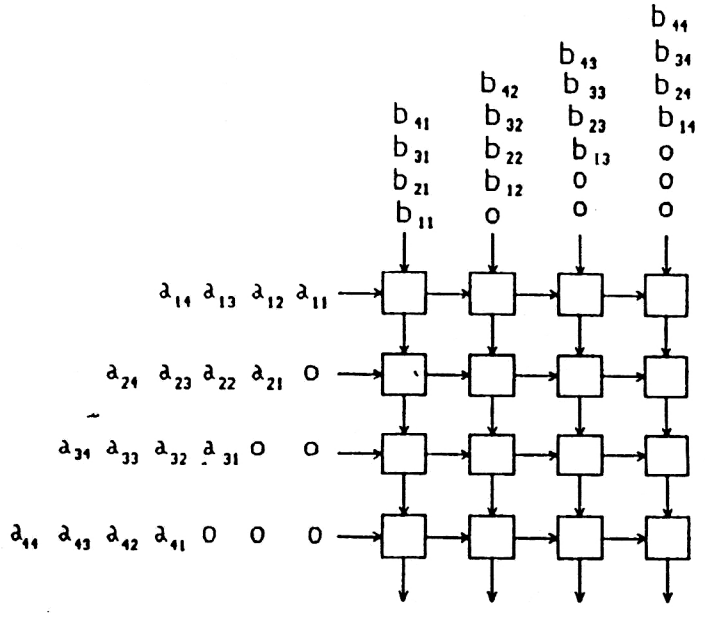

FIG. 21. Systolic array for realization of the multiplication of two matrices.

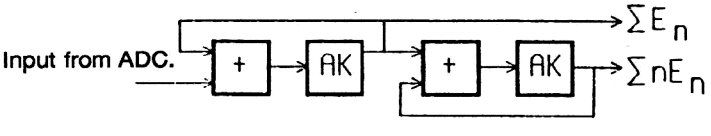

FIG. 22. Pipeline scheme for calculating the total energy and weighted sums.

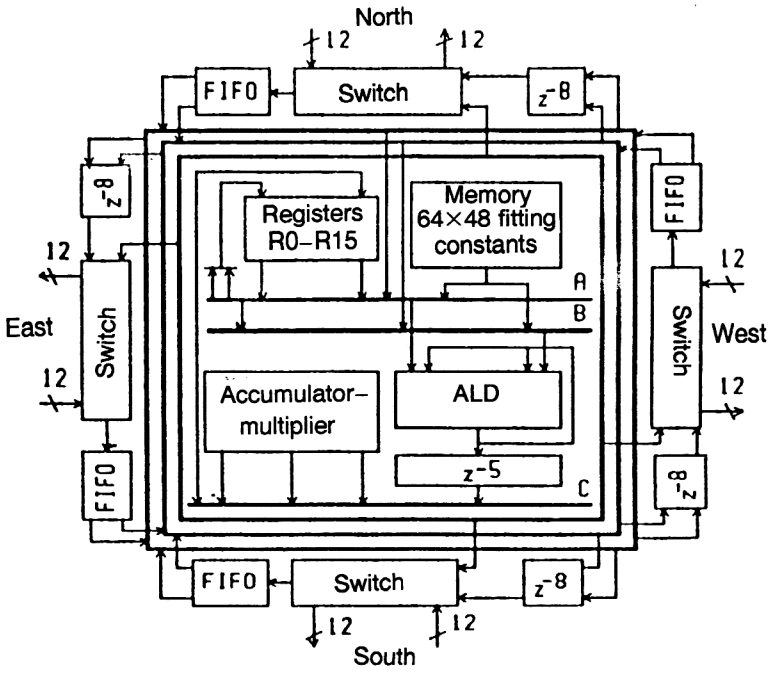

FIG. 23. Block diagram of wavefront processor.

experiments using the LHC accelerator. To avoid information loss during the period of collision of the beams, which is equal to 16 ns, it is necessary that each processor element of the systolic system be capable of processing the information that reaches it during 16 ns and transmit it to the nearest processor elements. The processor that has been developed works with clock frequency 67 MHz and belongs to the first-level trigger system.

The algorithm of the operation of the processor consists of three stages:

1) Identification of clusters in the electromagnetic calorimeter.

2) Adoption of a decision that a cluster is isolated.

3) Determination of the fact that the energy released in the corresponding cells of the hadronic calorimeter is low.

The data are sent to the systolic processor in a sequential code along 162 channels (81 inputs from the electromagnetic calorimeter and 81 from the hadronic part of the calorimeter). The systolic processor developed for LHC experiments[63] solves a wide class of problems: search for isolated electrons, muons, photons, and τ leptons, jets with high transverse momentum, leptons and jets; calculation of the transverse energy released by the effect of a neutrino or other interacting particles. The use a large number of sequential channels for the transfer and processing of data that operate in the pipeline regime makes it possible to solve in a simple manner one of the most difficult problems associated with the introduction of information into processor elements.

Wavefront arrays

One of the shortcomings of systolic architectures is that to control the data flow one needs strict synchrony and, as a consequence of this, additional time delays are introduced in the systolic array. As a result, the response time of the processor elements is inefficiently exploited, particularly if large processor arrays are used. Therefore a different approach to the construction of array processors is known in computational technology. It consists of replacement of strict synchrony by an asynchronous principle of interaction of processor elements by correct ordering of operations, as is done in flow computers or in wavefront arrays.[64] Wavefront processors acquired their name because there is a certain similarity between computational fronts and the fronts of electromagnetic waves, the principle of the propagation of which from point to point satisfies Huygens's law. Since the wavefronts of two successive recursions never intersect, the problem of conflict situations is simplified by means of registers or storage devices of the "first-in first-out" (FIFO) type. In wavefront arrays one still has the qualities of systolic arrays such as modularity and locality of the connections, linearity of the acceleration, and pipelinability. At the same time, there are some further qualities, above all the following: The triggering of a processor element depends only on the presence of the required operands and resources; there is a simpler representation of parallel operations, a large degree of pipelining of the computational process, and less use of the common memory and central control. However there are still problems in the connections between the memory blocks and conflicts when the memory is accessed. These factors influence the architecture of wavefront processors. Figure 23 shows a block diagram of a typical wavefront array processor,[65] which consists of processor elements and a common memory containing programs and information processing algorithms. The sequence of calculations begins at one element and then propagates in the form of waves over the complete array. Figure 24 shows the block diagram of a typical processor element (cell). It belongs to the class of processors in which an algorithm of many-data-and-many-commands type is realized. The basis of the wavefront processor element consists of 16 computers with RISK architecture (see below). Each cell interacts with four neighbors, except for the boundary cells, which can interact by means of

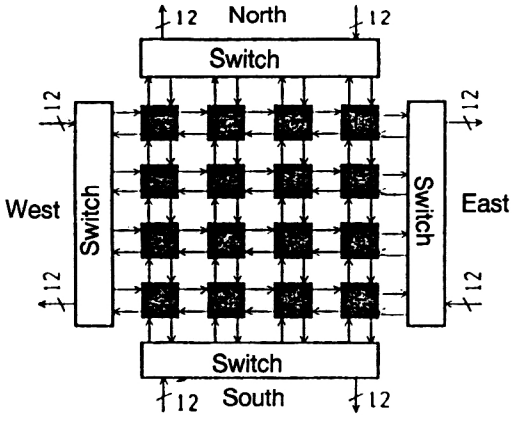

FIG. 24. Block diagram of processor element of wavefront processor.

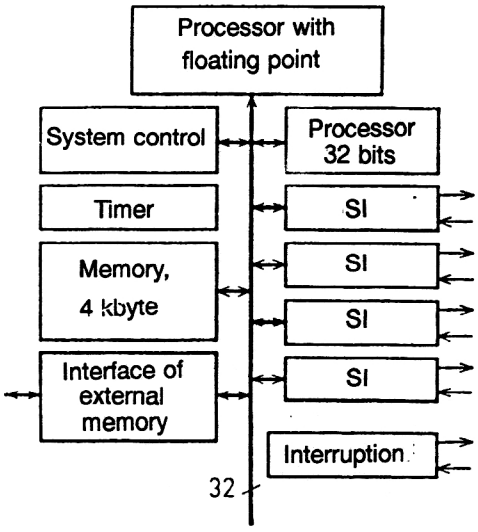

FIG. 26. Block diagram of the transputer T800. SI are sequential interfaces.

switches with four analogous wavefront processors by means of 12-digit words in the direction "north–east–south and west." The processor element adapted for pipeline data processing executes 250 MOPS, and the wavefront processor as a whole operates at a rate of 4000 MOPS. As is shown in Fig. 25, using just two analogous wavefront processors, it is possible to construct a one-dimensional cascade for the processing of 48-digit words.

RISK processor elements (Register-Intensive CPU)

Architecturally, a CPU is in essence a microcomputer on one crystal with 16-digit or 32-digit data highway. In contrast to universal computers that contain many commands and modifications of addresses that require much time for their implementation, in a CPU some of the most frequently encountered commands used in signal processing and in scientific calculations are foreseen. At the same time there is a maximum reduction of the forwarding of instructions by the use of registers and a fast immediate-access memory, which is in the same crystal with the processor. The commands themselves are arranged in the order of the frequency of their implementation. Register-intensive CPUs are of wide interest because they provide the basis of processors such as wavefront and signal processors and transputers. A CPU in a wavefront processor (Fig. 24) is surrounded by three annular data waves. The processor element consists of a multiplier–accumulator, an arithmetic–logic device (ALD), a register file, and program memory. The multiplier–accumulator executes multiplication of two 12-digit words, and the result is put in a 29-digit accumulator. The ALD operates in parallel with the multiplier. Between the dataway and the ALD, five buffer registers z^{-5} are introduced; these ensure consistency in the time of transfer of data from the ALD and the multiplier–accumulator. The presence of the buffer memory devices of FIFO type and shift z^{-8} registers, which perform a delay function, makes it possible for the wavefront processor to operate in the asynchronous regime. For clock frequency 125 MHZ, one processor element executes 250 MOPS. The technology of the manufacture of CPUs is progressing rapidly. Thus, in Ref. 66 there is a description of a 64-bit RISK processor of the firm MOTOROLA which also contains a graphical coprocessor, an associative buffer, etc.

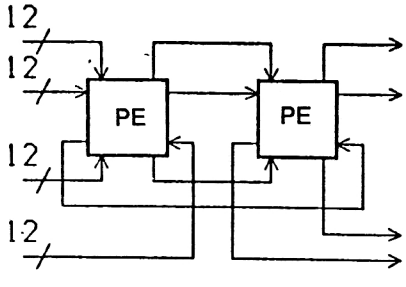

FIG. 25. One-dimensional 48-digit cascade formed from two 12-digit wavefront processor elements. PE are processor elements.

Transputers

The development of transputers made it possible to solve one of the most difficult problems in the construction of array processors—the guaranteeing of an effective connection between neighboring processor elements. The main difference between transputers and other microcomputers based on a single crystal is the presence of four successive duplex interfaces with high throughput (20 Mbits/s) and a very effective protocol. As processor in transputers one usually uses CPUs with different modifications. Figure 26 shows the block diagram of the transputer T800, which is used in experiments in high-energy physics.[67] Together with four sequential interfaces, the transputer T800 has a parallel 32-digit channel of direct access to an external memory. The immediate-access memory with capacity 4 kbyte, which is situated on the crystal, has the same access time as a file register. The computing power of the transputer is also ensured by a 32-digit processor with floating point. In addition, the transputer also contains a timer and backup schemes for external interruptions. The main command has a length of eight bits. Four bits are used to specify the codes of commands, and the remaining four bits are used for data coding.

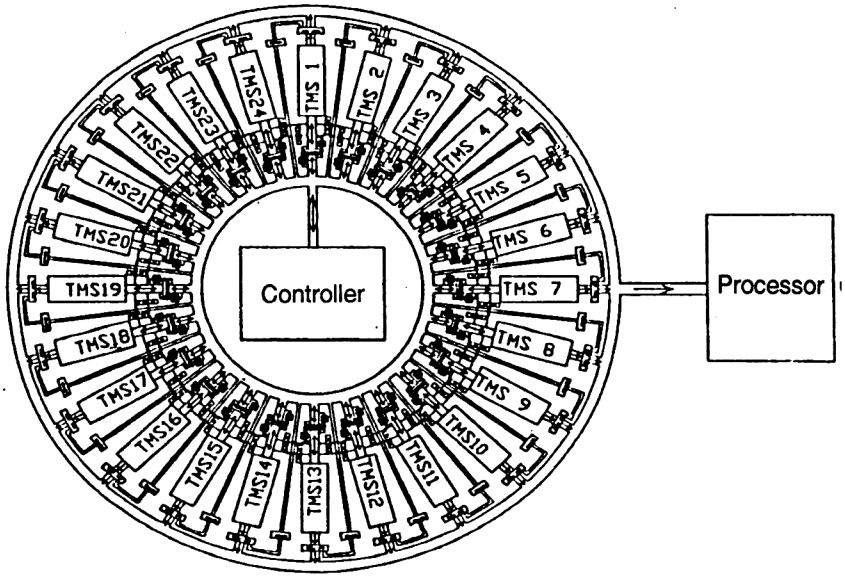

FIG. 27. Block diagram of trigger system of the calorimeter DELPHI. CC is the crate controller; MSP is the main signal processor; TMS1–TMS21 are signal processors.

There are also so-called prefix commands, by means of which it is possible to form rapidly operands of length greater than 15 bits. By means of transputers one can readily make parallel systems that are controlled by the specially created language Occam.[68] Transputers are widely used in the ZEUS facility.[69] Another example of the use of transputers is given in the interesting study of Ref. 70, which is devoted to the use of a neural network for the classification of e/π particles detected by means of a silicon calorimeter. Ultimately, it was necessary to separate electromagnetic showers from hadronic showers. For this purpose a powerful computational network was created, this including two transputers, a microVAX, an operating station and a personal computer. Modeling was done by means of the program GEANT 3.14.

Digital signal processors (DSPs)

The processors considered above can also be included in the class of signal processors. However, there can also be some differences. A DSP is a specialized microprocessor with instrumental architecture oriented toward the processing of digital signals, the sources of which may be, for example, ADCs. Some types of DSP can have their own built-in ADCs. A detailed review of signal processors and their use in high-energy physics experiments is given in Ref. 71. In order to increase the response time, such processors contain, as a rule, a separate memory for the program and data. The number of functions that can be performed is limited and is adapted above all for the implementation of operations such as parallel multiplication, cyclic shifts, manipulation with tabulated data, etc. Digital signal processors have been used for fast processing of signals detected in the calorimeter of the DELPHI facility.[72] The calorimeter contains 4500 lead-glass counters, which form 24 sectors. To each sector there is one corresponding processor (Fig. 27). The signal processor, receiving data from ADCs, subtracts pedestals, corrects numbers in accordance with given constants calculates the energy introduced in the sector, and compares it with an established threshold. All these operations are performed during 24 μs, this corresponding to the time of a second-level trigger. The processing of clusters is done in the third level of operation of the trigger system.

7. PROSPECTS FOR THE USE OF WAVEFRONT PROCESSORS IN THE SSC PROJECT

In this section we briefly consider the interesting project to develop a completely programmable first-level trigger for the calorimeter being constructed for the SSC. Various studies have been devoted to this question.[73–75] It is assumed that on the average 1.6 interactions can occur at the time of collision of the beams with a period 16 ns. The task of the trigger system will be to greatly reduce the level of background events. Every 16 ns, numerous subdetectors, including the calorimeter, will send data to the inputs of the first-level trigger to make a decision. The calorimeter will directly detect information relating to electrons, photons, particle jets, and energy losses E_t (from neutrinos). The calorimeter is shown schematically in Fig. 28. It is assumed that the total number of detection channels for the GEM experiment could be 60 000 for the electromagnetic part and 2000 for the hadronic part of the calorimeter. However it may also be possible here to reduce the number of channels by coarse graining the discreteness of the calorimeter "towers," as shown in Fig. 29. To separate the electrons and photons, the energy detected in the electromagnetic part of the calorimeter must be greater than a given threshold, and its ratio to the energy released in the hadronic part of the calorimeter must be a small quantity. In addition, the identification of an isolated cluster presupposes that the energy released in neighboring towers is also negligibly small. For the identification of particle jets, the total energy released in a tower is compared with a threshold. Neutrinos are identified similarly, namely, by measuring the sum E_t and making a comparison with a threshold value. It is proposed to use wavefront processors[73] to implement these conditions. There are two possible approaches to the realization of the conditions. The first method is based on the requirement that a cluster be distinguished under the condition that cells of a tower that are concentrated

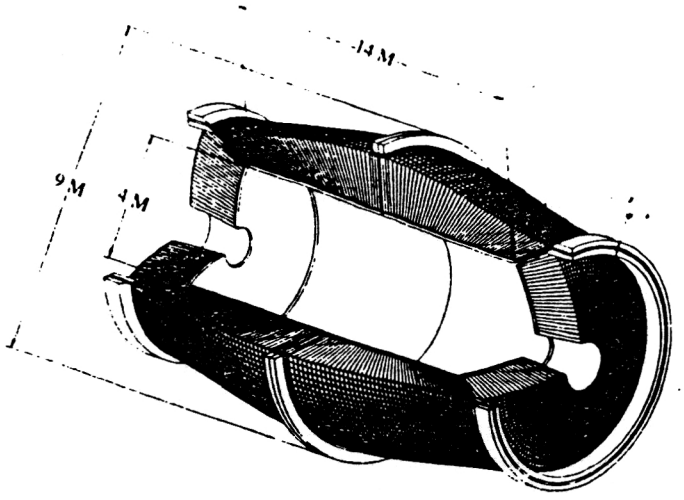

FIG. 28. Schematic drawing of calorimeter for experiments on the Superconducting Supercollider.

in a region of 3×3 cells have responded. The center of the cluster is found from the value of the local maximum (Fig. 30a), which is determined from the condition

$$C > I_i \quad \text{for } i = 1,2...8. \tag{2}$$

The sum of the energy of the tower and the eight neighboring towers must be greater than the threshold value:

$$\text{Threshold} < \sum_{i=1}^{8} I_i + C. \tag{3}$$

The algorithm of the search for electromagnetic clusters in a region of 4×4 matrices follows the aim of identification of electrons by comparing the sums from two neighboring towers with a threshold in a 1×2 or 2×1 region (Fig. 30b). A veto on the detection of an electromagnetic cluster can be imposed if there is an appreciable signal detected in the corresponding channel of the hadronic trigger or if the cluster candidate is not isolated, as shown in Fig. 31. In other words, the following conditions must be satisfied:

$$\text{Threshold} > \frac{C_h + I_h}{C_{em} + I_{em}},$$

$$\text{Threshold} < C_h + \sum_{i=1}^{3} I_h + \sum_{i=1}^{12} O_h + \sum_{i=1}^{12} O_{em}.$$

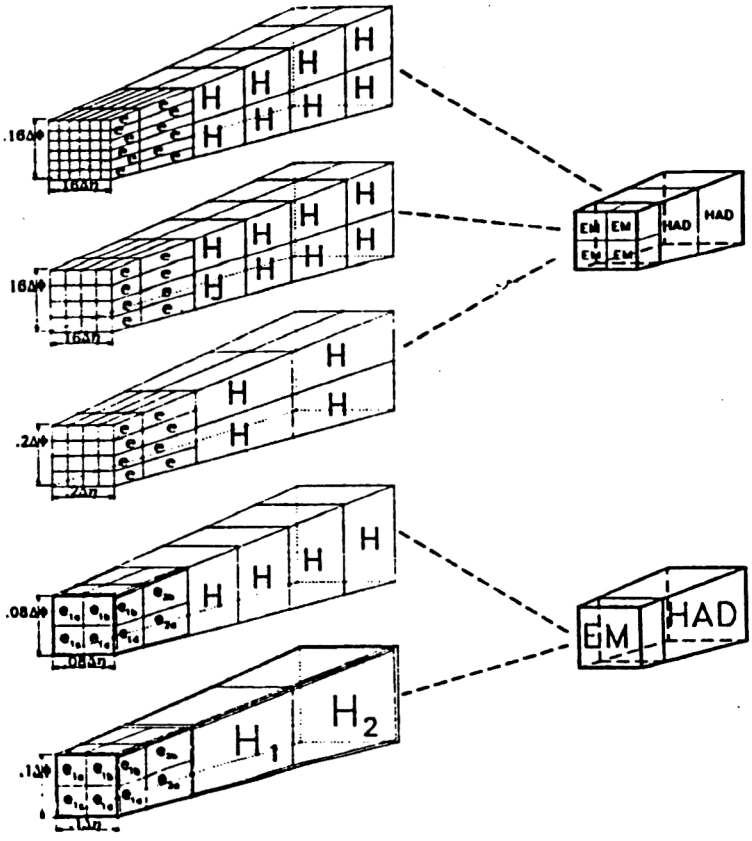

FIG. 29. Examples of different segmentations of calorimeter towers.

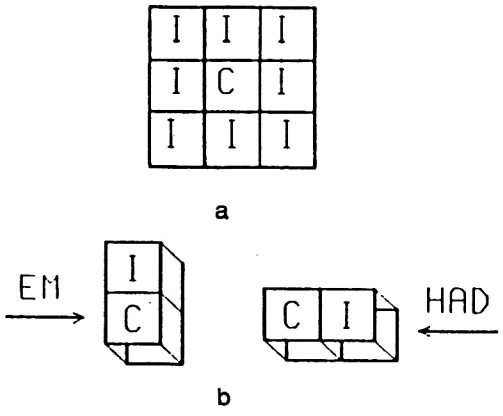

FIG. 30. Identification of local maximum (a); identification of electromagnetic clusters (b).

The search for jets is made in 4×4 and 8×8 regions (Fig. 32) with allowance for the condition

$$\text{Threshold} < \sum_{i=1}^{n} E_{em} + \sum_{i=1}^{n} E_h, \quad n = 16.64.$$

The array structure of the calorimeter dictated a choice of the signal processing system in which to each tower there corresponds a wavefront processor with structural scheme as shown in Fig. 23. As a result one then obtains overall a wavefront matrix processor system with high calculating rate that is moreover fully programmable. In such a system, each processor obtains data from neighboring towers and at the same time exchanges data operatively with adjacent processors. In the given study, the problems of feeding data into the processor elements and extracting data and the problems of programming the system are considered in detail. Figure 33 gives a generalized block diagram of the algorithm of the trigger system.

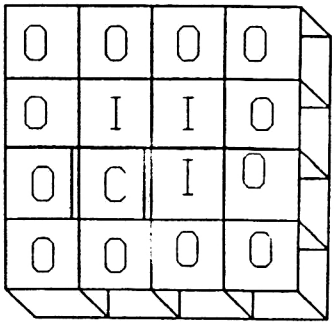

FIG. 31. Explanation of algorithm for finding isolated clusters.

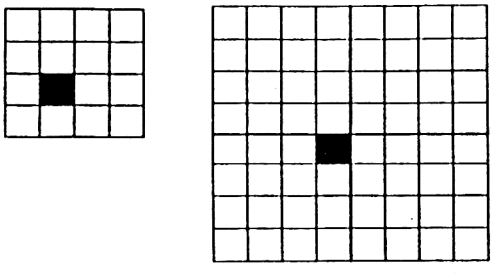

FIG. 32. Scheme of the search for particle jets in 4×4 and 8×8 arrays.

There was a further development of the fully programmable trigger for the *SSC* in the studies Refs. 74 and 75 of the same author in the form of the three-dimensional cellular architecture shown nominally in Fig. 34. The computational system, of the wavefront type, operates overall in an asynchronous regime. At the same time, individual processors (see Fig. 24) work with clock frequency 60–120 MHz. Together with four parallel interfaces, by means of which data are exchanged with neighboring wavefront processors in the directions "north, south, east, and west," the three-dimensional structure also effectively exploits two sequential interfaces with "up–down" directions, which are connected to annular dataways of each wavefront processor. These interfaces are mainly used to feed in programs, and also to monitor and debug the system. The data processing program begins to operate only when data are present at the inputs of the parallel interfaces. The presence of additional registers and a memory of FIFO type makes it possible to pump data uniformly from the calorimeter to the processors and minimize the operation implementation time. Four levels of implementation of the processing program can be identified (Fig. 34). In the first level, new data from the calorimeter are accepted simultaneously with the processing of the current information. After these data have been sent to the next level, the processor returns to implementation of the current program. The process of the calculations in the outputs of the processors proceeds in four stages, as for the input data. The final processor must produce a result every 16 ns. The study of Ref. 75 describes prototypes of three-dimensional (3*D*-Flow-Processor) 4×4 and 8×8 processors mounted on a printed circuit board and put together in the form of a cylindrical tower, as shown in Fig. 35. The data are carried from the calorimeter to the tower by means of optic fibers. Ventilators are arranged along the ends of the tower.

8. CLUSTER COUNTERS

It is often necessary simply to count the number of isolated clusters, including jet clusters. We now consider two algorithms that, judged in their totality, are equally effective. The essence of the first algorithm is the following.[76] We have the matrix

$$A = \begin{vmatrix} X_{1,1} & X_{1,2} & \cdots\cdots & X_{1,m} \\ X_{2,1} & X_{2,2} & \cdots\cdots & X_{2,m} \\ \cdots\cdots & \cdots\cdots & \cdots\cdots & \cdots\cdots \\ X_{n,1} & X_{n,2} & & X_{n,m} \end{vmatrix}.$$

Considering each current element of the matrix A as reference element, we calculate the values of Boolean expressions that contain, despite apparent complexity, four different variables:

$$S1_{n,m} = X_{n,m}\overline{X_{n+1,m}}. \tag{4}$$

In other words, in the expression (4) the number of units situated above a chosen reference point is calculated:

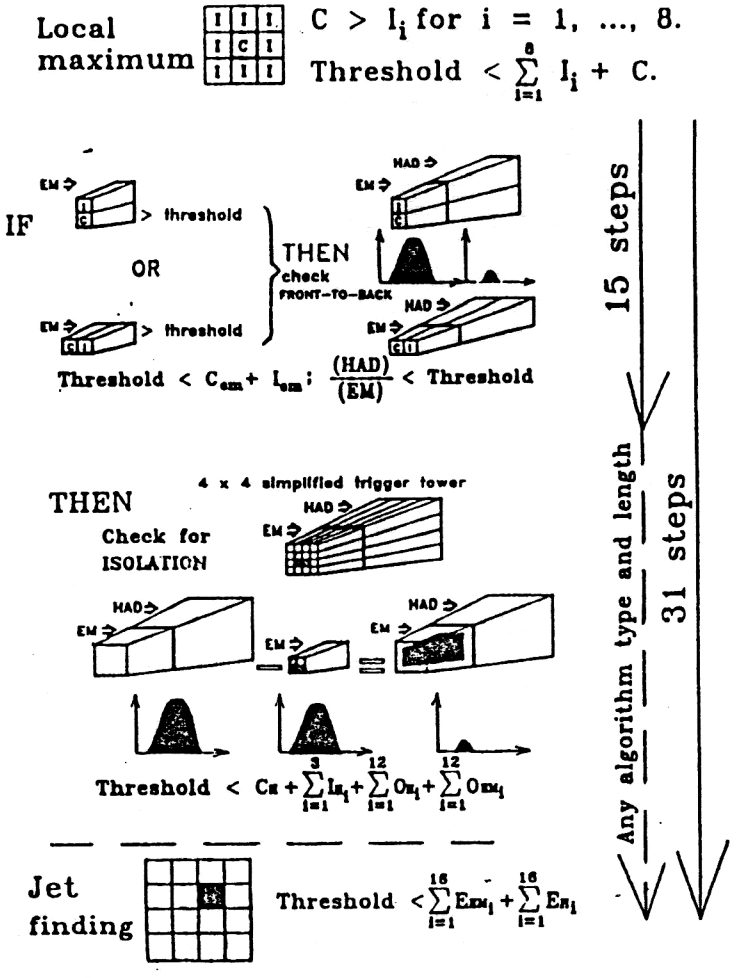

FIG. 33. Generalized scheme of the algorithm of operation of the trigger system.[73]

$$S2_{n,m}=\overline{X_{n,m-1}X_{n,m}}(X_{n+1,m}VX_{n+1,m-1}). \quad (5)$$

By means of the expression (5), a count is made of the number of units above the reference point plus above to the left and the absence of units to the left of the reference point. Then the number of clusters is

$$N_{c1}=\sum_{m=1}^{m}\sum_{n=1}^{n} S2_{n,m}-\sum_{m=1}^{m}\sum_{n=1}^{n} S1_{n,m},$$

At the same time, it is assumed that each element of the matrix A is placed in correspondence with a calorimeter counter.

In other words, the number of clusters is $S2-S1$. To simplify the exposition, we consider a simple example. Let $m=n=4$ and a cluster of the type

$$\begin{matrix} {}^{*}n,m \\ \times \\ \times \\ \times\times \end{matrix}$$

where * is the reference point and the crosses denote counters that have fired, be detected. We have

$$A=\begin{vmatrix} 0000 \\ 0100 \\ 0100 \\ 0110 \end{vmatrix}, \quad S1=\begin{vmatrix} 0100 \\ 0000 \\ 0010 \\ 0000 \end{vmatrix} \quad \text{and} \quad \sum S1=2.$$

It is easy to replace the value $S2_{n,m}=1$, and, in addition, for $k=m+1$ we have

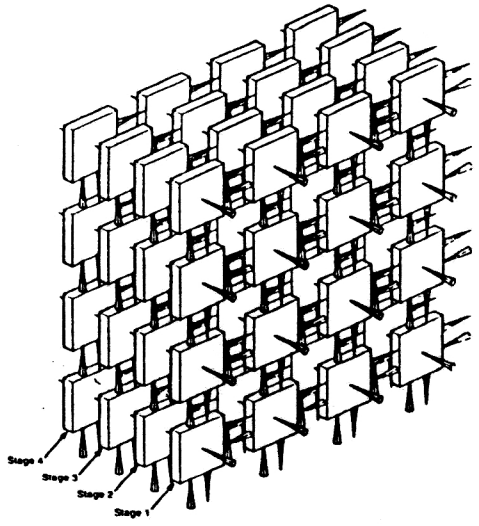

FIG. 34. General scheme of modernized three-dimensional pipeline computational system for first-level trigger.

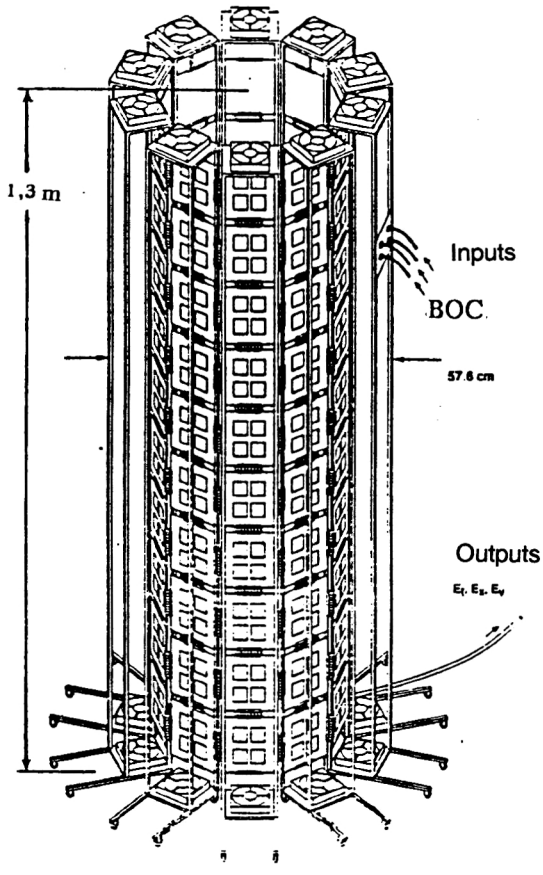

FIG. 35. General form of the constructed trigger system as assembled.

$$S2=\begin{vmatrix}0110\\0000\\0001\\0000\end{vmatrix} \quad \text{and} \quad \sum S2=3.$$

For the practical realization of the Boolean expressions (4)–(5), we can effectively use programmable logic arrays, and if the calculation for each point is made in parallel, then such a cluster counter can be used in the first-level trigger system. For a fast count of the number of units, parallel counters can be used.[77] Another algorithm is based on a count of the number of convexities and concavities in clusters, and it is sufficient to divide the obtained difference by four.[63] Thus, in the example that we consider above, the number of convexities is five, and there is one concavity.

9. USE OF THE METHOD OF SYNDROME CODING

It was shown above in specific examples that the number of counters in calorimeters can amount to tens of thousands, and the tendency to growth in the number of detection channels, like the complexity of the constructions, will continue strongly. As an example, we can mention the development of a calorimeter of "spaghetti" type,[78] by means of which it is planned to realize more effectively qualities of calorimeters such as the possibility of studying jets and their products, the identification of electrons, etc. From the methodological point of view,[78] the use of such calorimeters makes it possible to solve a number of problems that arise at superhigh energies: 1) the achievement of high radiation stability and a time resolution better than 15 ns; 2) a high energy resolution; 3) a short radiation length and small Molière radius; 4) a lowering of the cost. In the construction of detector prototypes that satisfy the requirements, lead glass is most frequently used as passive material, while bundles of scintillating optic fibers are used as the active medium. As an example, Fig. 36 shows the general form of a calorimeter prototype of the spaghetti type in section.[79] Each black hexagon is a section through a bundle of numerous optic fibers. Signal coding is therefore an important problem. Figure 37 shows the general form of a calorimeter module with preparatory coding,[80] in which planes consisting of scintillating optic fibers are interlayered with lead plates. To increase the accuracy of shower detection and reduce the number of photomultipliers, each plane is divided into six equal parts with ten fibers in each part. The light signals that arise in the fibers of the same orientation pass through mixers to the photomultiplier inputs. It will be shown below how the theory of error-correcting codes can be used for preparatory coding and compression of the data detected in the calorimeters by the use of iterative codes.

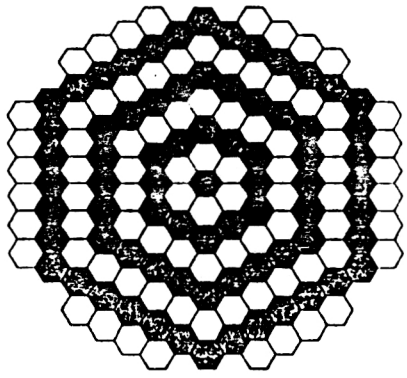

FIG. 36. Form in section of a spaghetti type calorimeter.

The use of iterative codes to construct parallel counters based on a large number of inputs was described by the

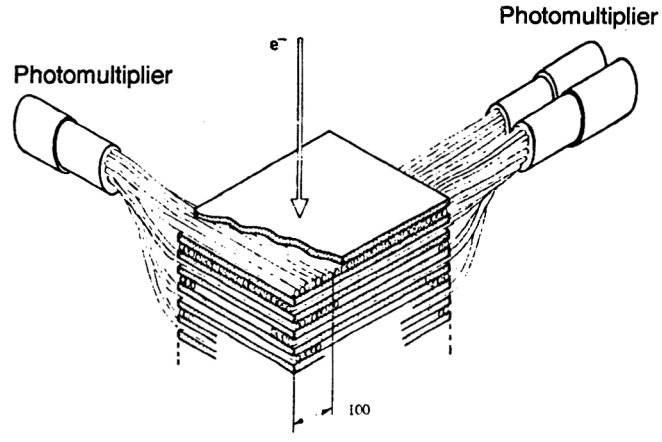

FIG. 37. Module of calorimeter with preparatory coding.

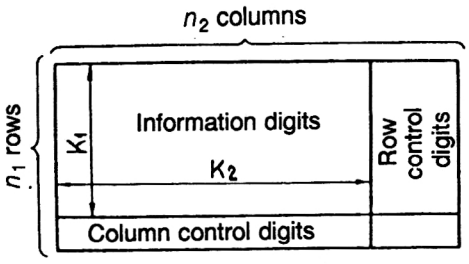

FIG. 38. Structure of two-dimensional iterative code.

present author in the review of Ref. 81. Such codes can also be used to detect clusters. The structure of a two-dimensional iterative code is shown in Fig. 38 (Ref. 82). Each information symbol is the symbol of combination of the two codes with the parameters (n_1,m_1,k_1,d_1) and (n_2,m_2,k_2,d_2). The resulting code is $n=n_1n_2$, $m=m_1m_2$, $k=k_1k_2$, and $d=d_1d_2$, where n, m, and k are code, information, and verification symbols, respectively; d is the code distance, which determines the correcting capability of the code. This quantity is related to the number t of errors that can be corrected by a simple relation that is known in the theory: $t=(d-1)/2$. In accordance with the method of syndrome coding, in our case t is the number of position-sensitive sensors in the detector that have fired, and m and n are equal to zero. Information about the event is contained in the syndrome code k. The task is, for given t, to find a coding scheme for which the number of bits in word k is a minimum. It can be seen from Fig. 38 that the structure of the two-dimensional iterative code has a certain similarity with the structure of hodoscope calorimeters and two-coordinate track detectors. Therefore, the use of such codes has great prospects for application and requires careful investigation.

In a number of cases, the algorithm for determining the coordinates and even the "images" of two-dimensional clusters can be simplified by transforming the clusters into individual lines (one-dimensional clusters), and by projecting the clusters onto the X and Y axes. We illustrate this by an example. Suppose a hodoscope calorimeter contains $29\times29=841$ counters, which are represented in the form of the two-dimensional matrix

												Y ↓
1	2	3	4	5	6	7	.....	26	27	28	29	0
30	31*	32*	33*	34	35	36	.....	55	56	57	58	1
59	60*	61*	62*	63	64	65	.....	84*	85*	86*	87	1
88	89*	90*	91*	92	93	94	.....	113*	114*	115*	116	1
117	118	119	120	121	122	123	.....	142*	143*	144*	145	1
.....	.....	.....	.....	.....	.....	.....	.....	.....	.....	.....	.....	...
784	785	786	787	788	789	790	.....	809	810	811	812	0
813	814	815	816	817	818	819	.....	838	839	840	841	0
0	1	1	1	0	0	0	.....	1	1	1	0	

$X\rightarrow$

Suppose that two isolated clusters have been detected and the data read out to registers corresponding to the two coordinates X and Y. The counters that have responded are indicated by the symbol *. As a result, we obtain a 58-digit word, by means of which, using programmable logic arrays or, reprogrammable memories, it is possible to determine rapidly from the presence of a gap in one of the "projections" the detection of two clusters. Unambiguous determination of the positions of two clusters in such a coding scheme is impossible, as is readily seen by considering two cases with diagonally conjugate events. These uncertainties can be eliminated if one introduces two additional tests along the diagonals, i.e., if one uses a four-dimensional iterative code with tests of "OR–OR" type. For a rough estimate of the value of k (without recourse to modeling), we can use the following theorems.[83]

1) For the detection by means of a code of length n all error packs of length b or less, it is necessary and sufficient to have b test symbols.

2) To correct (in our case detect) all error packs of length b or less a linear code must have at least $2b$ test symbols. For the correction of all error packs (clusters) of length b or less than $b<p$, a linear code must contain at least $b+p$ test symbols. We consider some examples. Iterative codes with tests of the type "OR–OR" and "even–even" are the simplest codes with sufficiently high compression coefficient.[84] However, such codes have a short code distance $d=4$. In Ref. 85 it was proposed to combine these codes, and it was shown how in this manner such a four-dimensional iterative code can be used to detect complicated events with clusters. As an example, Fig. 39 shows an event detected in a detector containing 1296 counters. The counters are represented in

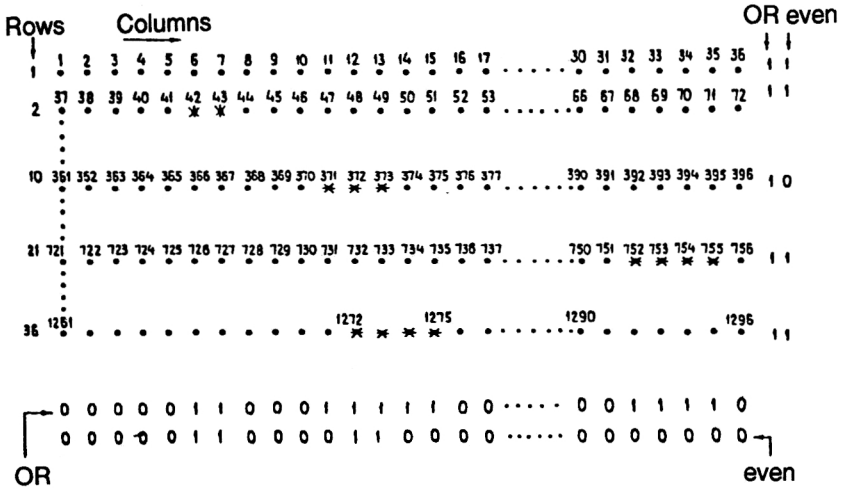

FIG. 39. Example of a complicated event recognized by means of a "even"–OR iterative code.

the form of an array consisting of 36 columns and 36 rows. It is easy to establish that the code syndrome is equal to 128 digits. We consider briefly an event recognition algorithm. Coincidence of "even" and "OR" signals in the first and second row and in the sixth and seventh column unambiguously indicates that pulses arrived from counters 6, 7, 42, and 43, etc. To increase the code distance, one can use additional diagonal tests or use for iteration codes with large code distances.

CONCLUSIONS

Calorimeters are very promising detectors that are used in experiments in the physics of high and superhigh energies. For the construction of total-absorption calorimeters and data processing, wide use is made of the most recent achievements of modern technology in fields such as cryogenic technology, semiconductor technology, optical methods of detection and processing of symbols, and the technology of fast specialized processors. In order to simplify the trigger systems, use is made of a number of constructional refinements that make it possible to create parallel channels for comprehensive selection of events with different physical processes. The number of physics problems that will be solved in the colliders that are under construction leads to the need to supply information detected in the calorimeters to the first-level trigger systems. Moreover, to ensure universality of the detector, the calorimeter triggers must be fully programmable. To solve such important problems, the developers of the instruments propose to use powerful array computational systems based on wavefront and systolic processors, programmable logic arrays, and neural networks.

It has been shown that for the fast selection of events with clusters it is expedient to use in a number of special cases preparatory data coding based on the method of syndrome coding. One can also pose the problem in a different plane: In accordance with the events expected for a given experiment, one should develop an optimum coding scheme containing the minimum number of digits in the syndrome code. It is to be expected that such a problem can be solved relatively easily by using the mathematical methods of modeling.

[1] T. Atkesson, M. Albrov, P. N. Burrows *et al.*, Preprint CERN-EP/87–88, Geneva (1987).
[2] B. N. Wiik, Preprint DESY 83–123, Hamburg (1983).
[3] P. Joos, Kerntechnik **56**, 242 (1991).
[4] N. L. Grigorov, V. S. Murzin, and I. D. Rapoport, Zh. Eksp. Teor. Fiz. **34**, 506 (1958) [Sov. Phys. JETP **7**, 348 (1958)].
[5] Yu. D. Prokoshkin, Preprint 79–148 [in Russian], Institute of High Energy Physics, Serpukhov (1979).
[6] C. W. Fabjan and R. Wigmans, Preprint CERN-EP/89-64 (1989).
[7] C. W. Fabjan and H. G. Fischer, Preprint CERN-EP/80-27, Geneva (1980).
[8] R. Wigmans, Preprint CERN-PPE/91-39, Geneva (1991).
[9] N. V. Rabin, Prib. Tekh. Eksp. No. 1, 12 (1992).
[10] N. V. Rabin, Prib. Tekh. Eksp. No. 6, 8 (1992).
[11] D. W. Hertzog, P. T. Debevec, R. A. Eisenstein *et al.*, Preprint Univ. of Illinois, NPL-91-002, Urbana (1991).
[12] P. Sonderegger, Nucl. Instrum. Methods **A257**, 523 (1987).
[13] T. Kamon, K. Kondo, and A. Yamashita, Nucl. Instrum. Methods **213**, 261 (1983).
[14] H. Fessler, P. Freund, K. M. Gelauer *et al.*, Preprint Max-Planck-Inst., MPI-PAE/Exp.E1.132, Munich (1984).
[15] P. Checchia, G. Galeazzi, U. Gasparini *et al.*, Nucl. Instrum. Methods **A248**, 317 (1986).
[16] A. M. Zaĭtsev, R. N. Krasnokutskiĭ, V. V. Lapin *et al.*, Preprint 92–154 [in Russian], Institute of High Energy Physics, Protvino (1992).
[17] H. Ikeda, M. Ikeda, T. Tanaka *et al.*, KEK Preprint, 90–134, Ibaraki-ken (1990).
[18] H. Ikeda, M. Ikeda, S. Inaba *et al.*, Nucl. Instrum. Methods **A292**, 439 (1990).
[19] K. Arisaka, J. Hauser, J. Kubic *et al.*, Preprint Univ. of California UCLA-HEP-90-007, Los Angeles (1990).
[20] W. Kononenko, W. Selove, G. E. Theodosiou *et al.*, Nucl. Instrum. Methods **214**, 237 (1983).
[21] R. Bartley, J. C. Berset, H. Breuker *et al.*, Preprint CERN-EP/85-91, Geneva (1985).
[22] C. Morell, Preprint Daresbury Lab. DL/SCI/TM62E, Daresbury (1989).
[23] J. E. Bateman, Nucl. Instrum. Methods **71**, 71 (1969).
[24] H. Dietl, G. Eigen, V. Fonseca *et al.*, Nucl. Instrum. Methods **A235**, 314 (1985).
[25] C. Bebek, Preprint Cornell Univ. CLNS 87/67, Ithaca (1987).
[26] W. Bruckner, M. Godberson, Kalakowsky *et al.*, Preprint CERN/PPE 91-146, Geneva (1991).
[27] H. Fenker and J. Thomas, Preprint SSC Lab. SSCL-611, Dallas (1983).
[28] S. G. Katvars, B. T. McCluskey, and J. M. Pentney, Nucl. Instrum. Methods **A276**, 482 (1989).
[29] S. Berglund, P. J. Carlson, and J. Jacobson, Nucl. Instrum. Methods **190**, 503 (1981).
[30] S. Bianco, P. Cantoni, P. Cotta-Ramusino *et al.*, Nucl. Instrum. Methods **A305**, 48 (1991).
[31] R. L. Chase, M. Dialinas, D. Fournier *et al.*, Preprint ORSE LAL 83/27, Orse (1983).
[32] P. N. Burrows, W. Busza, S. L. Cartwright *et al.*, Preprint Stanford Univ. SLAC-PUB-5305, Stanford (1990).

[33] A. Stevens, H. Kraner, V. Radeka *et al.*, Preprint Argonne Nat. Lab. ANL-HEP-CP-90-33, Argonne (1990).
[34] R. N. Krasnokutskiĭ, L. L. Kurchaninov, Yu. P. Petukhov *et al.*, Preprint OÉIUNK 91–16 [in Russian], Institute of High Energy Physics, Protvino (1991).
[35] G. Barbiellini, P. Buksh, G. Cecchet *et al.*, Preprint CERN-EP/84-139, Geneva (1984).
[36] E. Borchi, R. Macii, S. Mazzoni *et al.*, Preprint CERN-EP/89-28, Geneva (1989).
[37] S. A. Kleinfelder, IEEE Trans. Nucl. Sci. **NS-37**, 1230 (1990).
[38] G. Schuller, Preprint CERN 82–09, Geneva (1982).
[39] C. Blocker, G. W. Brandenburg, and R. Carey, Nucl. Instrum. Methods **216**, 71 (1983).
[40] K. S. Nelson and A. R. Erwin, IEEE Trans. Nucl. Sci. **NS-30**, 146 (1983).
[41] G. Zioulas, M. Arenton, T. Y. Chen *et al.*, Preprint Fermi Nat. Lab. Fermilab-Conf. 88/185-E, Batavia (1988).
[42] R. Ray, J. L. Rosen, M. Mazuzava, and J. Zhao, Preprint Fermi Nat. Lab. Fermilab-Pub-91/115, Batavia (1991).
[43] P. Bene, M. Bonesini, E. Bonvin *et al.*, Nucl. Instrum. Methods **A270**, 21 (1988).
[44] G. Stimple-Abele, Comput. Phys. Commun. **64**, 46 (1991).
[45] C. Lindsey and B. Denby, Preprint Fermi Nat. Lab. Fermilab-Pub-90/192, Batavia (1990).
[46] B. Denby, M. Cambell, F. Bedeschi *et al.*, Preprint Fermi Nat. Lab. Fermilab-Conf.-90/20, Batavia (1990).
[47] P. Bhat, L. Lonnblat, K. Meier *et al.*, Preprint DESY 90-144, Hamburg (1990).
[48] B. Denby, Comput. Phys. Commun. **49**, 429 (1988).
[49] C. Bortolotto, A. De Angelis, N. D. Groot *et al.*, Preprint INFN/AE-92/13, Trieste (1992).
[50] B. Denby, Preprint Fermi Nat. Lab. Fermilab-Conf.-90/94, Batavia (1990).
[51] B. Denby and S. Linn, Preprint Fermi Nat. Lab. FSU-SCRI-89-79, Batavia (1989).
[52] L. Gupta, A. M. Upadhye, B. Denby *et al.*, Preprint Fermi Nat. Lab. Fermilab-Pub-91/117, Batavia (1991).
[53] T. Altherr and J. C. Seixas, Preprint CERN-TH.5758/90, Geneva (1990).
[54] L. Lonnblad, C. Peterson, T. Rognvaldson *et al.*, Preprint Univ. of Lund. LU TP 90-8, Lund (1990).
[55] N. Bains, S. A. Baird, P. Biddulph *et al.*, Nucl. Instrum. Methods **A292**, 401 (1990).
[56] M. Abolins, D. Edmunds, P. Laurense, and Pi Bo, Nucl. Instrum. Methods **289**, 543 (1990).
[57] J. C. Browne, Phys. Today **37**, 28 (1984).
[58] Kung, Sun-Yuan, Proc. IEEE, **72**, 867 (1984).
[59] G. A. Kukharev, V. P. Shmerko, and E. N. Zaĭtseva, in *Algorithms and Systolic Processors for Processing Multiply Valued Data* [in Russian] (Navuka i Tekhnika, Minsk, 1990), p. 62.
[60] H. T. Kung, Computer **15**, 17 (1982).
[61] D. A. Paterson, Commun. ACM **28**, 8 (1985).
[62] G. Appelquist, B. Hovander, and B. Sellden, Preprint Stockholm Univ., No. USIP 92-04 (1992).
[63] C. Bohm, G. Appelquist, Xing Zhao, N. Yamdagni *et al.*, Preprint Stockholm Univ., No. USIP 92-08 (1992).
[64] Kung, Sun-Yuan, K. S. Arun, R. J. Gal-Ezer *et al.*, IEEE Trans. Comput. **C-31**, 1054 (1982).
[65] U. Shmidt and K. Caesar, IEEE MICRO 22 (1991).
[66] D. Berski, Elektronika **64**, No. 12, 8 (1992).
[67] T. Woeniger, Preprint DESY, No. 90-024, Hamburg (1990).
[68] J. G. Hey Antony, in *1988, CERN School of Computing*, CERN 89-06 (Geneva, 1989), p. 127.
[69] R. C. E. Devenish, Preprint University of Oxford and University College London, UK, OUNP-89-19 and ZEUS-89-76 (1989).
[70] P. Costa, Garlatti, and A. De Angelis, Preprint Università Di Udine–Istituto Di Fisika. No. 92/03/LS (1992).
[71] D. Crosetto, Preprint CERN. in *1990 CERN School of Computing*, CERN-91-05 (Geneva, 1991), p. 263.
[72] D. D. Crosetto, E. Menichetti, and G. Rinaudo, IEEE Trans. Nucl. Sci. **35**, 248 (1988).
[73] D. Crosetto and L. Love, Preprint SSC, No. SSCL-576, Dallas, July (1992).
[74] D. Crosetto, Preprint SSC, No. SSCL-165, Dallas, October (1992).
[75] D. Crosetto, Preprint SSCL-607, Dallas, December (1992).
[76] P. Illinger, Diplomarbeit.
[77] N. M. Nikityuk, Nucl. Instrum. Methods **A321**, 571 (1992).
[78] R. I. Dzelyadin, A. M. Zaitsev, A. A. Zaichenko *et al.*, Preprint IHEP 90-134, Protvino (1990).
[79] D. Acosta, S. Buontempo, L. Calooba *et al.*, Nucl. Instrum. Methods **A305**, 55 (1991).
[80] H. Burmiester, P. Sonderegger, J. M. Gago *et al.*, Nucl. Instrum. Methods **225**, 530 (1984).
[81] N. M. Nikityuk, Prib. Eksp. Teor. No. 1, 20 (1991).
[82] Ya. A. Khetagurov and Yu. P. Rudnev, *Improving the Reliability of Digital Devices by the Methods of Excess Coding* [in Russian] (Énergiya, Moscow, 1974), p. 35.
[83] W. W. Peterson, *Error-Correcting Codes* (MIT Press, Cambridge, Mass., 1962) [Russ. transl., Mir, Moscow, 1964].
[84] N. M. Nikityuk, Preprint R10-87-266 [in Russian], JINR, Dubna (1987).
[85] N. M. Nikityuk, in *Proc. of the Sixth Int. Conf., AAECC-6, Rome, Italy, July 1988*, edited by T. Mora, Vol. 357 (Springer-Verlag, Berlin, 1989), p. 324.

Translated by Julian B. Barbour